Mathematical Biosciences xxx (2014) xxx–xxx

Contents lists available at ScienceDirect

Mathematical Biosciences

journal homepage: www.elsevier.com/locate/mbs

Model selection for microbial nutrient uptake using a cost-benefit approach

J. Müller [a,b,*], B.A. Hense [b], S. Marozava [c], Ch. Kuttler [a,b], R.U. Meckenstock [c]

[a] Centre for Mathematical Sciences, TU München, Boltzmannstraße 3, D-85758 Garching, Germany
[b] Institute of Computational Biology, Helmholtzzentrum München, D-85764 Neuherberg, Germany
[c] Institute of Groundwater Ecology, Helmholtzzentrum München, D-85764 Neuherberg, Germany

ARTICLE INFO

Article history:
Received 11 January 2014
Received in revised form 5 June 2014
Accepted 18 June 2014
Available online xxxx

Keywords:
Bacterial substrate utilization
Optimization
Catabolite repression
Bistable nutrient uptake

ABSTRACT

We consider the uptake of various carbon sources by microorganisms based on four fundamental assumptions: (1) the uptake of nutrient follows a saturation characteristics (2) substrate processing has a benefit but comes at costs of maintaining the process chain (3) substrate uptake is controlled and (4) evolution optimized the control of substrate uptake. These assumptions result in relatively simple mathematical models. In case of two substrates, our main finding is the following: Depending on the overall topology of the metabolic pathway, three different behavioral patterns can be identified. (1) both substrates are consumed at a time, (2) one substrate is preferred and represses the uptake of the other (catabolite repression), or (3) a cell feeds exclusively on one or the other substrate, possibly leading to a population that splits in two sub-populations, each of them specialized on one substrate only.

Batch-culture and retentostat data of toluene, benzoate, and acetate uptake by *Geobacter metallireducens* are used to demonstrate that the model structure is suited for a quantitative description of uptake dynamics.

1. Introduction

Substrate utilization is a vital task of microorganisms that is tightly regulated. In batch culture, two substrates are often not consumed in parallel by bacteria, but the microorganisms prefer one over the other. Monod [28,15] observed this pattern the first time in *E. coli* which preferred glucose over lactose. This phenomenon was called carbon catabolite repression. The molecular basis of the corresponding regulatory pathway is well understood [44,12], and modeled in detail [1,3,4,46,48] (see also the review article of Santillán and Mackey [35] and references therein). These models identify many of the key players, and formulate their interplay with the aim of a quantitative, detailed description. However, in order to obtain data sets suited to identify the multitude of parameters, high throughput experiments measuring many components of the system are required. At the time being, this effort can only be afforded for a few, central pathways. Furthermore, details of many large models depend on the precise experimental setup in that different environments are likely to influence building blocks of the pathways in a way that is not straightforward to control.

In contrast to these detailed, large simulation models, simple conceptual models are developed to investigate the basic principle of microbial growth and substrate uptake, e.g. in chemostat [40,7,8], or for use in bioengineering [20,41,34]. For these two purposes, often simple models with few parameters have the clear advantage that theoretical and mathematical analysis is possible. Furthermore, only few parameters have to be estimated, rendering them attractive. As these parsimonious models formulate a prototypical structure, representing many different elements of a regulatory pathway in an averaging manner, they are likely to be rather stable against changes in the environment. The crucial point here is an appropriate specification of the model structure; results of models that do not use an adequate formulation are difficult to interpret. The selection of a feasible structure is only straight in simple situations. E.g., in case of several substrates, simple models often assume the parallel consumption [40,7], and disregard more complex regulation for substrate uptake.

So far, the mentioned approaches to investigate substrate uptake have been descriptive. Another approach is to analyse the rational behind the design of regulatory pathways or at least to take it into account. It is common believe that cells optimize their regulatory pathways in order to maximize their growth efficiency [43,38] and prevent to become out-competed by others. This general paradigm of evolution theory is non-trivial to use, as "efficient" is always to define with respect to a given environment

* Corresponding author at: Centre for Mathematical Sciences, TU München, Boltzmannstraße 3, D-85758 Garching, Germany. Tel.: +49 89289 18392.
E-mail address: johannes.mueller@mytum.de (J. Müller).

http://dx.doi.org/10.1016/j.mbs.2014.06.012
0025-5564/

that is subject to change; Metz et al. [27] show that certain requirements, which are not always satisfied, are necessary for the existence of an optimum. However, even simple assumptions about environment and optimality criteria can be helpful to comprehend observed regulatory networks. In [17,6], the *lac* operon is analyzed with respect to its efficiency in certain scenarios (constant lactose concentration, and fluctuating environments). The authors conclude that this operon is optimized, indeed. Similar arguments can be found e.g. in [11,32], also for the consumption of other sugars. Another approach uses adaptive dynamics to decide about the optimal allocation of different resources in ecological models [36,45]. These ecological oriented papers do not focus on regulatory mechanisms but investigate phenomenological allocation strategies.

The aim of the present article is to reverse the concept: instead of starting off with existing regulatory pathways, describing them and investigating their efficiency, we start off with few assumptions about the topology, costs, and benefits of a metabolic pathway. The optimization principle then predicts relatively simple models for microbial substrate uptake and growth. We claim that this approach automatically leads to appropriate models. In that, the present work is close to metabolic control theory due to Kascar et al. [16] and cybernetic modeling of metabolic fluxes [20,41,34].

In the spirit of the simple models mentioned above, we use the developed theory twofold: in a qualitative way, as a conceptual model to comprehend the basic principles ruling the control of substrate uptake, and in a quantitative way, as a tool for bioengineering. We are on the one hand able to derive a classification of certain interaction patterns, and relate them to biochemical principles. On the other hand we are able to model experiments for the uptake of toluene, benzoate, and acetate by *Geobacter metallireducens*. This is an environmentally relevant anaerobic microorganism. It is known to degrade aromatic pollutants in the groundwaters including toluene and it is also able to use easily degradable substrates present in the environment, e.g. acetate [23]. The results of modeling indicate that the present approach is indeed suited to be used in practical applications.

2. Modeling of efficiency of metabolic pathways

Our starting point are four basic assumptions about microbial metabolic pathways:

(1) the uptake of nutrient follows a saturation characteristics
(2) substrate processing has a benefit but comes at costs of maintaining the process chain
(3) substrate uptake is controlled
(4) evolution optimized the control of substrate uptake.

These four fairly general statements are substantiated below by means of mathematical equations. The aim is to use these four assumptions in order to select a model for a given pathway. We will first consider the most simple situation – one substrate only, and then proceed to the case that several substrates are present. Necessarily, the assumptions made induce certain shortcomings. In particular, assumption (4) – the optimization – will be done with respect to a constant environment, considering individual cells only. Later we will discuss which aspects we miss by this constrain.

2.1. One substrate

First we analyse the situation of a single cell, processing one single substrate that is available at a concentration u constant in time. In order to formulate the control for substrate uptake, a variable describing the state of this control, or the potential activity of the pathway, is required; we name this variable α (see Table 1 for the variables used). While u relates to the environment, α relates to the internal state of a given cell. The variable α represents the overall readiness to process the substrate – *if* there is substrate ($u > 0$), cells will consume it at a rate given by α and u; *if* there is no substrate ($u = 0$), the cell may nevertheless be prepared to take up the substrate. Therefore α represents the *potential* activity or the control. In response to the environment, the cell will dynamically adapt this control. In order to be less abstract, we could think of α to represent the number of transport molecules in the cell membrane. Once the substrate is transported into the cell, it will be utilized by the particular pathway. It should be emphasized that this thought model for α is not meant as a recipe for measurements of the potential activity level, but rather as a theoretical concept helping to gasp the idea behind α. Indeed, α represents in an averaging manner all components used to control a pathway, including uptake and degrading enzymes. This variable allows to quantify two different aspects: firstly, it is related to the rate at which a substrate is consumed, and secondly it allows an overall estimation of the costs connected with the maintenance of the pathway at a given potential activity level.

Growth is the read-out that is to optimize. Growth indicates in some sense the energy available to the cell. That is why we will also call this optimization the maximization of energy. Let $\mathcal{E}_{cell}$ be the complete energy available. This energy is the sum of several gain and loss terms. Some of the (for us) most relevant terms will be discussed now. Assumption (1) indicates that the consumption of a substrate follows a saturation function. The most natural saturation function is a Monod term in αu. The substrate degraded is converted into biomass production or growth rate. The benefit $\mathcal{E}_+(\alpha; u)$ of the substrate available at a level αu

$$\mathcal{E}_+(\alpha; u) = \frac{\mu_{max}\,\alpha\, u}{K_s + \alpha\, u}, \tag{1}$$

quantifies the contribution to the growth rate, or energy (see also Fig. 1). As usual, μ_{max} indicates the maximal possible benefit, and K_s the value for αu at which we find the half-maximal benefit. The interpretation developed so far requires that the activity assumes non-negative values, $\alpha \geqslant 0$.

Apart from the benefit, there is a second effect connected with α: microorganisms need to maintain the pathway at a certain level of activity, which comes with costs. As we want to keep things as simple as possible, we assume that these costs increase linearly in α with proportionality constant e, and define the corresponding contribution $\mathcal{E}_-(\alpha)$ to the net growth rate by

$$\mathcal{E}_-(\alpha) = -e\,\alpha. \tag{2}$$

Note that this term does not include direct costs for processing nutrient. $\mathcal{E}_-(\alpha)$ are merely the maintenance costs for the metabolic pathway at a certain activity level, that are even there if the corresponding nutrient is not available. We may interpret this assumption as follows: in order to keep a certain activity level, a certain

Table 1
Abbreviations and meaning for the conceptual model.

Name	Unit	Interpretation
u	Mol	Concentration of nutrient
α	1/Mol	Activity/metabolic control variable
$\mathcal{E}$	biomass/h	Contribution of the pathway to the growth rate
$\mathcal{E}_+$	biomass/h	Energy gain by actual nutrient uptake
$\mathcal{E}_-$	biomass/h	Energy loss by maintenance of the pathway
K_s	1	Rescaled half-saturation of the monot kinetic
μ_{max}	biomass/h	maximal degradation rate
e	biomass/(h u)	Proportionality constant between activity and costs

Q1 Please cite this article in press as: J. Müller et al., Model selection for microbial nutrient uptake using a cost-benefit approach, Math. Biosci. (2014), http://dx.doi.org/10.1016/j.mbs.2014.06.012

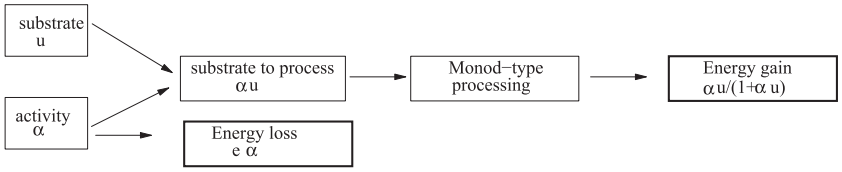

Fig. 1. Structure of the energy gain/energy loss for one pathway.

number of e.g. transport proteins have to be sustained. These proteins are degraded at a certain rate γ, say, and have to be replaced at the same rate. If each protein costs n energy units (an appropriate measure for "energy units" could be for example the number of ATP molecules used for the production of one protein), the energy lost per time unit is $n\alpha\gamma$. With $e = n\gamma$ we find the term for $\mathcal{E}_-(\alpha)$ above. As α represents all parts of the pathway, the interpretation may be more complex, but the description given here shows the principle behind the assumed shape of $\mathcal{E}_-(\alpha)$.

The total growth rate of a cell of course depends on a multitude of factors: maintenance, temperature, availability of other substrates and molecules apart from the substrate under consideration (e.g. electron acceptors), the pH in the environment, etc. For now, we assume that all these influences do not change, and are either additive or multiplicative to the pathway under consideration, but do not directly depend on u and α. That is, we assume that the overall net growth rate $\mathcal{E}_{cell}$ is given by

$$\mathcal{E}_{cell} = \mathcal{E}_{cell,0} + A(\mathcal{E}_+(\alpha;u) + \mathcal{E}_-(\alpha)). \tag{3}$$

where $\mathcal{E}_{cell,0}$ and A may depend on many influences, but are assumed to be independent on α and u, i.e. independent on the pathway under consideration. Furthermore, $A > 0$. We now believe that the cell optimizes the control, i.e. maximizes $\mathcal{E}_{cell}$. As $\mathcal{E}_{cell,0}$ and A are constant and $A > 0$, this is equivalent with the maximization of

$$\mathcal{E}(\alpha;u) := \mathcal{E}_+(\alpha;u) + \mathcal{E}_-(\alpha) = \frac{\mu_{max}\,\alpha u}{K_s + \alpha u} - e\,\alpha. \tag{4}$$

To be precise in notation, we will call $\mathcal{E}$ the net (energy) gain, while we call $\mathcal{E}_+$ the (energy) gain, and $\mathcal{E}_-$ the costs (of this pathway).

Most likely, the special forms of the functional responses chosen here do not matter for the discussion below. Important are two features: an unbounded, strictly monotonous increasing maintenance costs $\mathcal{E}_-(\alpha)$, and a monotonously increasing saturation function in αu that describes the gain $\mathcal{E}_+(u;\alpha)$.

We may simplify the expression: defining $\tilde{\alpha} = \alpha/K_s$ and $\tilde{e} = eK_s/\mu_{max}$, we find

$$\frac{\mu_{max}\,\alpha u}{K_s + \alpha u} - e\,\alpha = \mu_{max}\left(\frac{\tilde{\alpha} u}{1 + \tilde{\alpha} u} - \tilde{e}\,\tilde{\alpha}\right). \tag{5}$$

This is, a reparameterization allows to take μ_{max} and K_s to one. For now, we will stay with this parametrization and drop the tilde again. We assume that the regulatory network in the cell is designed in such a way that the control variable α is adjusted to maximize the energy intake. In consequence, either $\alpha = 0$ if $\mathcal{E}(\alpha;u)$ is a monotonously decreasing function in α, or α is given by a local maximum,

$$0 = \frac{\partial}{\partial\alpha}\mathcal{E}(\alpha;u) = \frac{u}{(1+\alpha u)^2} - e \iff \alpha = \frac{1}{u}\left(\sqrt{\frac{u}{e}} - 1\right). \tag{6}$$

If this term is negative, $\mathcal{E}$ is monotonously decreasing for all $\alpha \geqslant 0$ and the optimal activity level α in this case is zero. This is, the optimal strategy $\alpha^* = \alpha^*(u)$ in presence of a constant (time-independent) substrate concentration u can be written as

$$\alpha^*(u) = \frac{1}{u}\left(\sqrt{\frac{u}{e}} - 1\right)_+, \tag{7}$$

where we define the brackets $(\cdot)_+$ by $(x)_+ = x$ for $x > 0$ and $(x)_+ = 0$ else. The energy gain reads

$$\mathcal{E}(\alpha^*(u);u) = \left(\left(1 - \sqrt{\frac{e}{u}}\right)_+\right)^2. \tag{8}$$

The control variable is positive only for $u/e > 1$. This threshold can be interpreted as follows: if α is small, then $\alpha u/(1+\alpha u) \approx \alpha u$. If we identify α with the concentration of transport proteins, each of these proteins yield a gain of u energy units per time unit. On the other hand, each of these proteins costs e energy units per time unit. The net gain is positive, if $u > e$. Only in this case, it pays to process the substrate.

2.2. Two substrates

It may be of value to keep in mind that the model developed here will be applied to experiments looking at the uptake of toluene, acetate and benzoate. That is, we are interested in the interactions of metabolic pathways processing different substrates.

Pathways processing two substrates eventually converge, as they have to end in central building-blocks for biomass production, e.g. pyruvate or acetyl-CoA. We find the first part of the processing chains to go in parallel, more or less independent of each other. Eventually the paths merge into one single processing route. Which setups are interesting? The main difference in the pathways addressed here is the location of bottlenecks. Bottlenecks represent the capacity-limiting biochemical step in the pathway (modeled by a Monot term). Bottlenecks may be indicated by intrinsic costs, either to produce the corresponding enzymes (in the spirit of the "potential activity"), or to process the substrate. Basically, we identify three different situations (see Fig. 2): (a) the bottlenecks are located in the parallel parts, above the convergence point. In this case, the pathways will not or only weekly influence each other. We name this topology "independent pathways". (b) No bottleneck is located upstream of the convergence point, but only downstream. This is the "early convergence" situation. We will model the combination of benzoate and acetate in this way. Acetate is converted in acetl CoA, and benzoate is first converted to bezoyl-CoA, which in turn is transformed to acetyl CoA (see Fig. 6). The data indicate that these conversions happen rather readily, and therefore no bottleneck is identified in this part of the pathway.

(c) Only one of the substrates possesses a bottleneck upstream of the converging point, and a further bottleneck is located downstream. One substrate flows without hindrance to the converging point, while the other first passes an obstacle. Basically all nutrient without upstream bottleneck is available in the convergence point. This structure allows to re-interpret this situation slightly, in assuming that one of the substrates is converted into the other one, and subsequently they are commonly processed. This topology is called the "hierarchical" situation. We use this pattern to formulate the submodel for toluene and benzoate. Toluene is converted into benzoyl CoA, and so is benzoate. However, the growth data indicate that the conversion of toluene requires a considerable higher effort than the conversion of benzoate. This observation suggests the hierarchical topology for these two substrates.

Q1 Please cite this article in press as: J. Müller et al., Model selection for microbial nutrient uptake using a cost-benefit approach, Math. Biosci. (2014), http://dx.doi.org/10.1016/j.mbs.2014.06.012

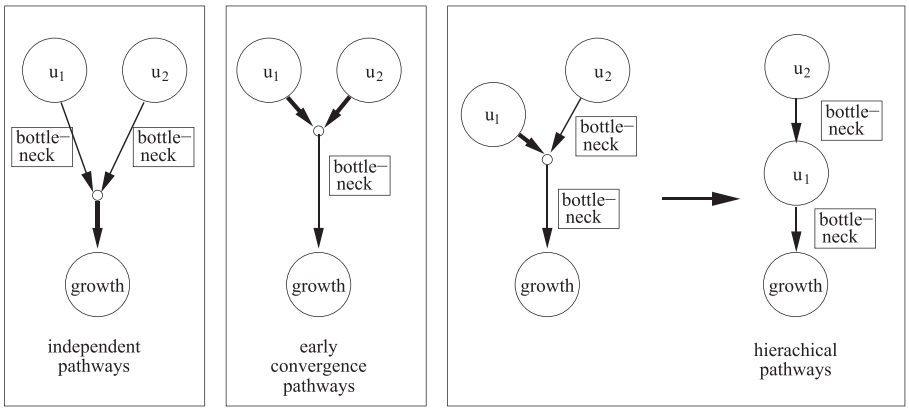

Fig. 2. Different topologies considered in case of two pathways. Bold arrows indicate the non-limiting parts, slim arrows the limiting parts (also called bottle-necks) of the metabolism.

In the next subsections, we discuss the different control pattern emerging from these topologies.

2.2.1. Independent pathways

Let us consider two pathways that work independently, in a parallel mode. We attach an index $i \in \{1,2\}$ to all variables to indicate pathway one or pathway two. The net energy for each of the two paths is given by

$$\mathcal{E}_i(\alpha_i;u_i) = \frac{\alpha_i u_i}{1+\alpha_i u_i} - e_i\,\alpha_i. \tag{9}$$

These two net energies have to be combined to one single term. Thereto, we weight the gain, using substrate one as reference. $\mathcal{E}_2$ is multiplied by a constant θ,

$$\mathcal{E}(\alpha_1,\alpha_2;u_1,u_2) = \mathcal{E}_1(\alpha_1;u_1) + \theta\mathcal{E}_2(\alpha_2;u_2). \tag{10}$$

θ indicates the different energy yield per unit of u_2 in comparison with u_1: if $\theta > 1$, the energy gain per molecule u_2 is larger, if $\theta \in (0,1)$, it is less than that of u_1. Clearly, as the two pathways are independent, the optima for the pathways are those of the individual pathways,

$$\alpha_i^*(u_1,u_2) = \frac{1}{u_i}\left(\sqrt{\frac{u_i}{e_i}} - 1\right)_+, \tag{11}$$

with the total energy

$$\mathcal{E}(\alpha_1,\alpha_2;u_1,u_2) = \left(\left(1-\sqrt{\frac{e_1}{u_1}}\right)_+\right)^2 + \theta\left(\left(1-\sqrt{\frac{e_2}{u_2}}\right)_+\right)^2. \tag{12}$$

We may identify different regions in the plane given by the normalized substrate concentrations u_1/e_1 and u_2/e_2; in each of these regions, we find another optimal strategy (α_1,α_2). We call this figure bifurcation diagram, although – strictly spoken – we have no dynamics and hence no bifurcations in the sense of dynamical systems. However, we will later introduce dynamics and are therefore allowed to interpret the diagrams as bifurcation diagrams. The bifurcation diagram for the given topology is depicted in Fig. 3. In the upper, left part of the figure, for different combinations of u_1/e_1 and u_2/e_2, different regions are indicated. E.g., if $u_1/e_1,\ u_2/e_2$ is small, the combination falls in the region named A. In order to read off the optimal strategy, we go to the small diagrams below the two larger panels: Here, we find a α_1,α_2 coordinate system, with a bullet located in the point $\alpha_1 = \alpha_2 = 0$. This dot indicates, that the strategy $\alpha_1 = \alpha_2 = 0$ is optimal in the region A. If we increase u_1/e_1 above one but stay with u_2/e_2 below one, we move to region C_1. Again, in the α_1,α_2 panels we find one named C_1; here we have a black dot at $\alpha_2 = 0,\ \alpha_1 > 0$. That is, the optimal strategy for the cell is to consume substrate u_1 only. Additionally to the bullet we also find an open circle. Later, we will introduce dynamics. The open circles indicate unstable, stationary states (saddle points in the energy landscape, or minima/maxima if we restrict ourselves to the axes, but the landscape increases if we go into the interior of the positive cone). The region D is interesting: here, we find a bullet in the interior of the positive quadrant, indicating that the optima for α_1 and α_2 are strictly positive. If there is sufficient substrate, both substrates are consumed in parallel. As we have no direct influence of one pathway on the other pathway, both are degraded if there is enough substrate s.t. the degradation pays.

2.2.2. Early-converging pathways

In case of the topology called "early converging pathway", the pathways soon converge into a single one with limited capacities. We model this effect by

$$\mathcal{E}(\alpha_1,\alpha_2;u_1,u_2) = \frac{\alpha_1 u_1}{1+\alpha_1 u_1+\alpha_2 u_2} - e_1\,\alpha_1 + \theta\left(\frac{\alpha_2 u_2}{1+\alpha_1 u_1+\alpha_2 u_2} - e_2\,\alpha_2\right). \tag{13}$$

There are the trivial cases that $u_1/e_1 < 1$ indicating that it does not pay to degrade substrate one (regions A, B_1 in Fig. 3), resp. $u_2/e_2 < 1$ (regions A, C_1 in Fig. 3), s.t. substrate two is not utilized. If $u_1/e_1, u_2/e_2 > 1$, the situation is non-trivial, as each substrate alone pays to be degraded. Only interactions may hinder a substrate from being consumed. A more detailed analysis partially based on numerical observations (Appendix A) reveals that several cases are to be distinguished: in C_2 and E, there is a (local) optimum where substrate one is degraded alone, while in B_2 and E there is a local optimum where substrate two is degraded alone. The regions B_1 and B_2 can be interpreted as catabolite repression; if θ is not close to one (i.e., the substrates have a rather different yield), the region E is narrow and close to one axis. I.e., B_2 is large and C_2 small, or vice versa, indicating that the inhibition is not symmetrical, one of the substrates is overwhelming predominant. We know this situation from glucose and lactose.

If the yield of the substrates are similar, $\theta \approx 1$, then E may become large (see also Fig. 11). It is not merely a small strip, separating the regions where one substrate clearly dominates the other, but we expect also in experiments (or in nature) the substrate concentrations to meet this region. The two local optima that are present in region E indicate that a given cell has to decide between two different favorable strategies: either to only feed on substrate one, or to only feed on substrate two. Of course, generically, only one of these strategies forms a global optimum, while

Q1 Please cite this article in press as: J. Müller et al., Model selection for microbial nutrient uptake using a cost-benefit approach, Math. Biosci. (2014), http://dx.doi.org/10.1016/j.mbs.2014.06.012

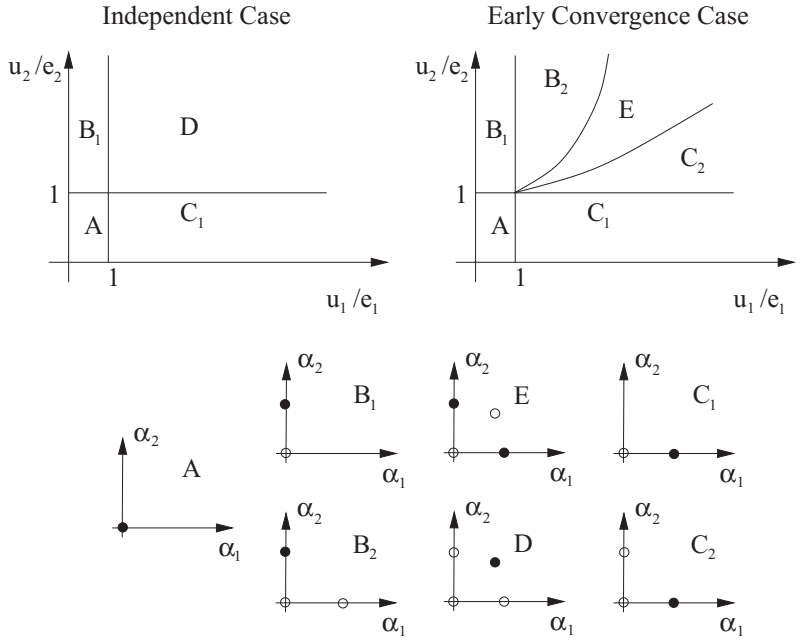

Fig. 3. Bifurcation diagram for the case of independent pathways (first row, left panel) and early converging pathways (first row, right panel). The bold lines indicate transcritical bifurcations, while the dashed line in the right panel denotes a global bifurcation. Panels below indicate the optima in the different regions of the parameter space. Bullets indicate local maxima, open circles extremal points that fail to be local maxima (minima or saddle points).

the other one only is a local optimum. In this sense, all cells should go for the global optimum. Cells are faced with the difficult problem to avoid local maxima and select the global maximum.

It is inspiring to briefly review the mathematical theory of optimization. There are two fundamentally different approaches. One class uses local information to improve a candidate solution of an optimization problem by small steps. A typical member of this class is the method of steepest ascent: the candidate solution is shifted along the gradient of the target function. Such methods approach efficiently the next local maximum. They completely depend on the initial conditions. If the starting point is close to the global optimum, they are likely to converge to that. If local maxima are closer, they will not converge to the global maximum, but select a local maximum. Another class is formed by stochastic methods. A typical member here is simulated annealing. Randomly a new candidate solution is chosen, and accepted at a certain probability. It is even allowed – with a relatively small probability – that the next candidate solution is worse than the present one. In this way, the algorithm prevents to get stuck in a local maximum. Under certain conditions, it is possible to prove that the global optimum is found almost surly. These class of algorithms is relatively slow, but much better suited for a rough energy landscape. It is most likely that hybrid algorithms, combining local and deterministic parts with some global, stochastic component, are the most powerful optimizers for a wide range of target functions.

Based on these considerations, we expect that cells move towards one of the two local maxima; stochastic components of the biochemical pathway controlling substrate uptake will lead to a heterogeneous population, where a fraction of cells choose the "substrate-one-only" solution, while the other fraction selects the "substrate-two-only" solution. The exact distribution of the population cannot be determined taking the view of a single cell only, but by consideration of the overall population; most likely it also depends on the typical time course of the substrate concentrations in the environment. We expect that arguments similarly to those indicating the optimality of bed-hedging in case of switching environment [29] can be used to analyse the present situation. It is out of the scope of the present work to follow this line of thoughts.

2.2.3. Hierarchical pathways

Now we come to a situation that is *per se* not symmetric any more: the hierarchical topology (see Fig. 4). The second substrate (concentration u_2) is first transformed to the first substrate (concentration u_1) and then – using the pathway of the first substrate – converted to energy. Such a pathway design is frequently found, e.g. if beside monosaccharides as glucose their oligo- or polysaccharides as cellulose, starch or cellobiose are used for nutrition, or in the stepwise degradation of aromatic pollutants [24,37]. We adapt our basic model to allow for this intertwined situation.

For u_1, the situation does not change: in case $u_2 = 0$ we have one pathway of the usual type. This part is well described by the net energy gain

$$\mathcal{E}_1(\alpha_1; u_1) = \frac{\alpha_1 u_1}{1 + \alpha_1 u_1} - e_1 \alpha_1. \tag{14}$$

In case of the second substrate, u_2, we have a first step that converts substrate two into substrate one, and then pathway one is used. We denote by U_2 the concentration of the intermediate product, i.e. of substrate u_2 that has been converted into a form that can be handled by pathway 1 in the same way like u_1. This first step in the metabolism of u_2, the conversion into U_2, may be connected with gain as well as loss of energy. We presume that in this conversion step a bottleneck is present. In accordance with earlier considerations the rate at which U_2 is produced is given by

$$\frac{\alpha_2 u_2}{1 + \alpha_2 u_2}. \tag{15}$$

For convenience, we denote by e_3 the loss of energy superimposed by this first degradation step; each molecule converted requires e.g. a certain number of ATP molecules, i.e. comes at some costs. It may happen, of course, that during this first step ATP molecules are produced, and we have a given energy gain per molecule converted; this case is covered by taking e_2 to negative values. The contribution of this step to the net gain is described by $-e_3 \alpha_2 u_2/(1 + \alpha_2 u_2)$. The product of this first step is assumed to

Q1 Please cite this article in press as: J. Müller et al., Model selection for microbial nutrient uptake using a cost-benefit approach, Math. Biosci. (2014), http://dx.doi.org/10.1016/j.mbs.2014.06.012

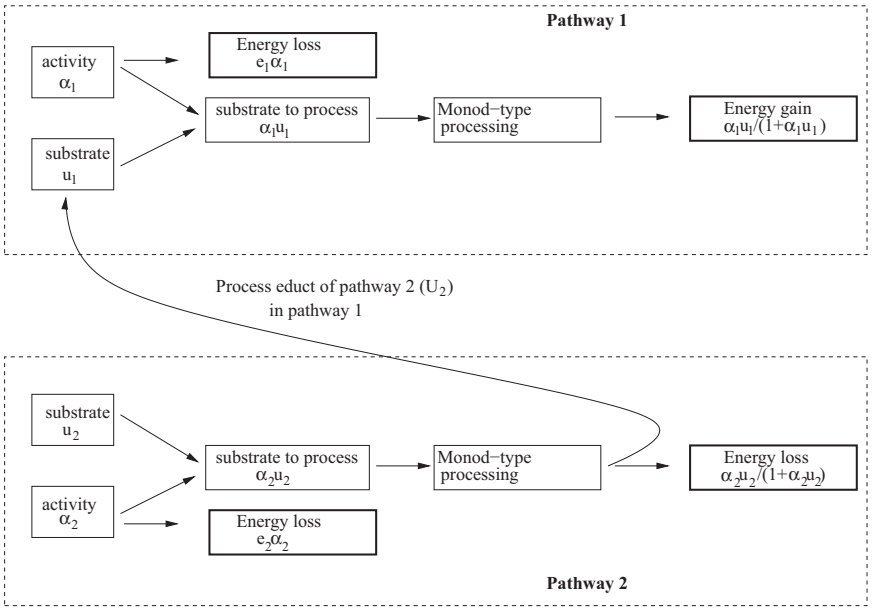

Fig. 4. Two serial pathways. Nutrient two (concentration u_2) is converted into an intermediate product (concentration U_2), which is fed into the pathway of nutrient one (concentration u_1).

be equivalent with substrate one, and fed into the substrate-one-processing-chain in the same way as substrate one. The overall net energy gain reads

$$\mathcal{E}(\alpha_1,\alpha_2;u_1,u_2)=\frac{\alpha_1(u_1+U_2)}{1+\alpha_1(u_1+U_2)}-e_3\frac{\alpha_2u_2}{1+\alpha_2u_2}-e_1\alpha_1 - e_2\alpha_2. \tag{16}$$

How can we obtain the concentration U_2? In the present considerations, we focus on an equilibrium situation. U_2 should be produced at the same rate at which it is further processed,

$$\frac{\alpha_2u_2}{1+\alpha_2u_2}=\frac{\alpha_1U_2}{1+\alpha_1(u_1+U_2)}. \tag{17}$$

Solving this equation for U_2, we find

$$\alpha_1U_2=\left(\frac{\alpha_2u_2(1+\alpha_1u_1)}{1+\alpha_2u_2}\right)\left(1-\frac{\alpha_2u_2}{1+\alpha_2u_2}\right)^{-1} =\alpha_2u_2(1+\alpha_1u_1). \tag{18}$$

Using these two relations, we obtain the overall net gain

$$\mathcal{E}(\alpha_1,\alpha_2;u_1,u_2)=\frac{\alpha_1u_1}{(1+\alpha_1u_1)(1+\alpha_2u_2)}-e_1\alpha_1+(1-e_3) \times\frac{\alpha_2u_2}{1+\alpha_2u_2}-e_2\alpha_2. \tag{19}$$

In view of our applications, we concentrate on the case $e_3>0$. The energy gain per molecule of substrate u_2 is smaller than that for substrate u_1, as the pre-processing is connected with costs. From the formula for the net gain, we read-off that for $e_3>1$ it never pays to utilize u_2. If $e_3>1$, we are left with $\alpha_2=0$ and a single-pathways-situation for u_1. As this situation is already well understood, we restrict ourselves to $e_3\in(0,1)$.

The analysis can be found in Appendix B, partially performed by numerical analysis only. We summarize the outcome in Fig. 5 and in the following statement:

Result: The overall structure of the bifurcation diagram resembles that of the early convergence case: the regions A, B_1, B_2, C_1 and C_2 are similar; only the region E in the early convergence pathway is split into several sub-regions in the present case. The reason for this similarity is the similarity of the topology: once the intermediate product U_2 is formed, we basically have an early-convergence topology for u_1 and U_2.

The analysis indicates that two cases have to be distinguished: $e_3\in(0,3/4)$ and $e_3\in(3/4,1)$. The bifurcation diagrams are slightly different for these two cases. However, in both cases we find that for u_1 large, and u_2 small enough, the trivial solution $\alpha_2=0$ is a local maximum of the energy gain function (parameter regions C_1, C_2). Under these conditions, substrate u_1 will prevent substrate u_2 from being processed. If the concentration of u_1 decreases, eventually it pays to utilize u_2. Inspecting the bifurcation diagram, the concentration of u_1 has to be rather small until the degradation of substrate two is beneficial. This situation can be interpreted as catabolite repression. The details for the transition from utilization of u_1 only (C_2) to the utilization of u_2 only (region B_2) depends on the energy necessary to pre-process u_2. If this energy is large, i.e. $e_3\in(3/4,1)$, we have a region (D_1) resembling heterogeneous region of the early-convergence pathway. In this region, the strategies given by degradation of one substrate only form two local optima. It is likely to find a heterogeneous population. In the other case, where the effort for the pre-processing is not very high, i.e. $e_3\in(0,3/4)$, the transition from C_2 (substrate one only) to B_2 (substrate two only) happens via parallel degradation of both substrates: in D_2 as well as in E, there is an optimal strategy in the interior of the cone. Both substrates are consumed in parallel. However, in E and F, we still have the possibility of heterogeneity, as two local optima are present at the same time.

3. Dynamic models

In real world situations, substrate concentrations are likely to change in time. We add dynamics to the models above. At the same time, we slightly extend the concept to become more realistic: we take into account the possibility of a constant, low basal degradation, caused e.g. by co-metabolic degradation. In this section, we focus on the applicability of the models developed, and not on a classification of behavioral types as we did on the last section. The equations developed here will be used to analyse batch- and retentostat data.

Q1 Please cite this article in press as: J. Müller et al., Model selection for microbial nutrient uptake using a cost-benefit approach, Math. Biosci. (2014), http://dx.doi.org/10.1016/j.mbs.2014.06.012

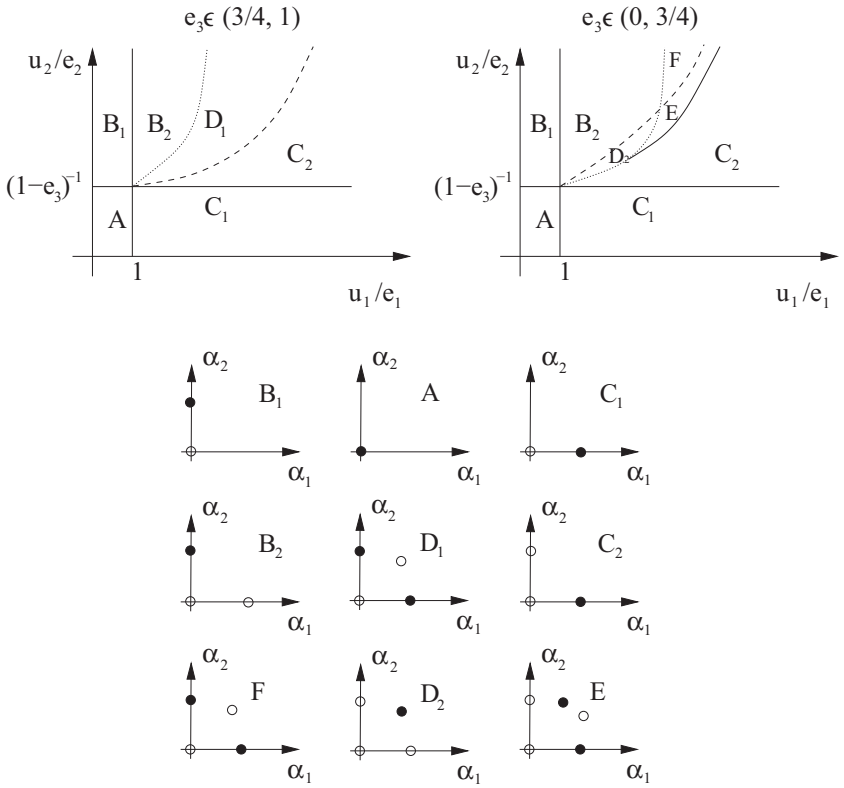

Fig. 5. Bifurcation diagram for $e_3 \in (3/4, 1)$ (upper row, left) and $e_3 \in (0, 3/4)$ (upper row, right). If $e_3 \geqslant 1$, we always find $\alpha_2 = 0$. The bold dashed and dotted lines in the parameter plane denote transcritical bifurcations, the dashed-dotted line (right panel) represents the line of saddle-node bifurcations. For the interpretation of circles and bullets in the panels below see caption of Fig. 3.

3.1. Single substrate

Let $p(t)$ denote the population size (density), $u(t)$ the substrate concentration, and $\alpha(t)$ the activity of the pathway at time t. Note that we implicitly assume a homogeneous population – all cells use the same substrate consumption strategy $\alpha(t)$. The net energy gain given in Eq. (4) describes population growth as well as substrate uptake – the growth is due to conversion of substrate into biomass. In accordance to the standard chemostat models, we assume at the present time that the costs (for the pathway as well as for maintenance) are small and can be neglected to describe the population growth with the precision necessary to analyse data. Growth-rate and substrate uptake rate are proportional to the energy gain $\mathcal{E}_+(\alpha; u) = K\alpha u/(K_m + \alpha u)$, with proportionality constants A resp. B,

$$P' = A\left(\frac{K\,\alpha u}{K_m + \alpha u}\right)p \quad \text{and} \quad u' = -B\left(\frac{K\,\alpha u}{K_m + \alpha u}\right)p. \tag{20}$$

The more sophisticated (and, in some sense, more arbitrary) part is the formulation of the dynamics for the control variable α. Given the substrate concentration u, this variable should adapt to the optimal value discussed above. The variable should always climb to higher net energy levels, leading to the equation $\alpha' = \partial_\alpha \mathcal{E}(\alpha, u)$. The control variable α is assumed to stay non-negative. In order to force the equation to preserve positivity, we replace the r.h.s. by $\alpha\partial_\alpha \mathcal{E}(\alpha, u)$. Two more aspects are included: first, we allow for a basal degradation. The costs for this basal degradation are part of the general maintenance costs, and do not count for $\mathcal{E}_-(\alpha; u)$. We rewrite the costs of the pathway as

$$\mathcal{E}_-(\alpha; u) := e(\alpha - \alpha^0)_+ \tag{21}$$

where, as before, $(x)_+$ is zero if $x < 0$, and $(x_+) = x$ for $x > 0$. That is, if the control variable α becomes less than a minimal activity α^0, the costs drop to zero; since only the term $-e(\alpha - \alpha^0)_+$ has a negative contribution to α' and becomes zero for $\alpha \leqslant \alpha^0$, there will be always a basal, minimal activity of the pathway. In some cases, this basal activity may be interpreted as co-metabolic degradation. The last point that we take into account is the time scale of adaptation, expressed by ε. All in all, we derive at

$$\varepsilon\alpha' = \alpha\partial_a(\mathcal{E}_+(\alpha; u) - \mathcal{E}_-(\alpha)) = \alpha\partial_a\left(\frac{K\,\alpha u}{K_m + \alpha u} - e(\alpha - \alpha^0)_+\right). \tag{22}$$

If ε is small enough, we may apply Fenichels theory; i.e., the system is well approximated by assuming the quasi steady state $\alpha(t) = \alpha^*(u(t))$. This assumption leads to a two-dimensional system of equations

$$p' = A\mathcal{E}_+(\alpha^*(u); u)p = Af(u)\,p, \quad u' = -B\mathcal{E}_+(\alpha^*(u); u)p = -Bf(u)\,p. \tag{23}$$

The function $f(u)$ possesses the typical properties usually assumed for the term describing the uptake rate of substrate: $f(0) = 0, f(u)$ is monotonously increasing, and $f(u)$ is bounded. In this, the model we derived here by considering optimization of energy uptake basically yields the usual model for microorganisms consuming substrate in a batch culture. The present approach is consistent with well tested models [40].

3.1.1. Independent pathways

The considerations for one pathway can be directly generalized to this case. If we take into account a basal degradation, we find the net energy gain given by

$$\mathcal{E}(\alpha_1, \alpha_2, u_1, u_2) = \big(\mathcal{E}_{1,+}(\alpha_1; u_1) - e_1(\alpha_1 - \alpha_1^0)_+\big) + \theta\big(\mathcal{E}_{2,+}(\alpha_:, u_2) - e_2(\alpha_2 - \alpha_2^0)_+\big), \tag{24}$$

where the terms $\mathcal{E}_{i,+}(\alpha_i,u_i)=\alpha_i u_i/(K_i+\alpha_i u_i)$ reflect the substrate uptake, and θ indicate the different energy content in the two substrates. The control variables will climb upwards towards an optimization of the energy gain (along the gradient), and we find/define the equations ruling the dynamics of the control variables similar to the case with one substrate only,

$$\begin{aligned}
p' &= A_1\mathcal{E}_{1,+}(\alpha_1;u_1)p + A_2\mathcal{E}_{2,+}(\alpha_2;u_2)p\\
u_1' &= -B_1\mathcal{E}_{1,+}(\alpha_1;u_1)p\\
u_2' &= -B_2\mathcal{E}_{2,+}(\alpha_2;u_2)p\\
\varepsilon_1\alpha_1' &= \alpha_1\partial_{\alpha_1}\mathcal{E}(\alpha_1,\alpha_2,u_1,u_2) = \alpha_1\partial_{\alpha_1}\big(\mathcal{E}_+(\alpha_1;u_1) - e_1(\alpha_1-\alpha_1^0)_+\big)\\
\varepsilon_2\alpha_2' &= \alpha_2\partial_{\alpha_2}\mathcal{E}(\alpha_1,\alpha_2,u_1,u_2) = \theta\alpha_2\partial_{\alpha_2}\big(\mathcal{E}_+(\alpha_2;u_2) - e_2(\alpha_2-\alpha_2^0)_+\big).
\end{aligned} \tag{25}$$

If $\varepsilon_i \ll 1$, we may reduce the equations to two dimensions by assuming α_i to be in their quasi-steady state. As in the case of one substrate only, we obtain $p' = (A_1f_1(u_1)+A_2f_2(u_2))p$, $u' = (B_1f_1(u_1)+B_2f_2(u_2))p$, where $f_i(u)$ have similar characteristics as a Monod function. We obtain a model structure that resembles the usual two-substrate-models for e.g. the chemostat [7].

3.2. Two substrates

3.2.1. Early converging pathways

The dynamic model equations for the early converging pathway resemble those for the parallel pathways; we only need to take the interaction into account in defining

$$\mathcal{E}_{i,+}(\alpha_1,\alpha_2;u_1,u_2) = \frac{u_i\alpha_i}{1+(u_1\alpha_1+u_2\alpha_2)}. \tag{26}$$

The net gain reads

$$\begin{aligned}
\mathcal{E} = \mathcal{E}_{1,+}(\alpha_1,\alpha_2;u_1,u_2) - e_1(\alpha_1-\alpha_1^0)_+ + \theta(\mathcal{E}_{2,+}(\alpha_1,\alpha_2;u_1,u_2)\\
- e_2(\alpha_2-\alpha_2^0)_+).
\end{aligned} \tag{27}$$

The full, dynamic model is given by Eq. (25) with the obvious changes. This model is able to address more complex behavior as catabolite repression.

3.2.2. Hierarchical pathways

Recall the structure of the present topology: substrate u_1 is degraded directly, basically following the one-substrate case. The second substrate u_2 is first converted into an intermediate product U_2, that is subsequently degraded by the u_1-pathway in the early-convergence-fashion (competition of u_1 and U_2 in the bottleneck of the u_1-pathway). The model equations are obvious (with the notation introduced above in Section 2.2.3); we only add the time scale η for the dynamics of the intermediate product U_2,

$$\begin{aligned}
p' &= A_1(\mathcal{E}_{+,1,1}(\alpha_2;u_1,U_2)+\mathcal{E}_{+,1,2}(\alpha_2;u_1,U_2)) + A_2\mathcal{E}_{+,2}(\alpha_2;u_2)\\
u_1' &= -B_1\mathcal{E}_{+,1,1}(\alpha_2;u_1,U_2)\,p\\
u_2' &= -B_2\mathcal{E}_{+,2}(\alpha_1;u_2)\,p\\
\eta U_2' &= \hat{B}_2\mathcal{E}_{+,2}(\alpha_1;u_2)\,p - \check{B}_2\,\mathcal{E}_{+,1,2}(\alpha_2;u_1,U_2)\,p\\
\varepsilon_1\alpha_1' &= \alpha_1\partial_{\alpha_1}\mathcal{E}(\alpha_1,\alpha_2,u_1,u_2,U_2)\\
\varepsilon_2\alpha_2' &= \alpha_2\partial_{\alpha_2}\mathcal{E}(\alpha_1,\alpha_2,u_1,u_2,U_2)\\
\mathcal{E}_{+,1,1}(\alpha_1,\alpha_2;u_1,U_2) &= \frac{\alpha_1u_1}{1+\alpha_1(u_1+U_2)},\\
\mathcal{E}_{+,1,2}(\alpha_1,\alpha_2;u_1,U_2) &= \frac{\alpha_1U_2}{1+\alpha_1(u_1+U_2)}\\
\mathcal{E}_{+,2}(\alpha_2;u_2) &= \frac{\alpha_2u_2}{1+\alpha_2u_2}\\
\mathcal{E}(\alpha_1,\alpha_2;u_1,u_2,U_2) &= \mathcal{E}_{+,1,1}(\alpha_1,\alpha_2;u_1,U_2)\\
&\quad - e_1(\alpha_1-\alpha_1^0)_+\theta\big[\mathcal{E}_{+,1,2}(\alpha_1,\alpha_2,u_1,U_2) - e_2(\alpha_2-\alpha_2^0)_+\\
&\quad -e_3\mathcal{E}_{+,2}(\alpha_2;u_2)\big].
\end{aligned} \tag{28}$$

The factor θ scales the energy yield of the two pathways. In order to simplify the model, we take η to zero, assuming the quasi-steady state for U_2. There is no justification for this assumption; experience shows that in many cases the resulting model is suited to explain data. With $B=\hat{B}_2/\check{B}_2$ we find in the quasi-steady state

$$B\frac{\alpha_2u_2}{1+\alpha_2u_2} = \frac{\alpha_1U_2}{1+\alpha_1(u_1+U_2)}. \tag{29}$$

Solving this equation for U_2

$$\alpha_1U_2 = \frac{(1+\alpha_1u_1)(\alpha_2u_2)}{1+(1-B)\alpha_2u_2} \tag{30}$$

yields the system

$$\begin{aligned}
p' &= A_1\mathcal{E}_{+,1}(\alpha_1,\alpha_2,u_1,u_2) + A_2\mathcal{E}_{+,2}(\alpha_1,\alpha_2,u_1,u_2)\\
u_1' &= -B_1\tilde{\mathcal{E}}_{+,1}(\alpha_1,\alpha_2;u_1,u_2)\,p\\
u_2' &= -B_2\tilde{\mathcal{E}}_{+,2}(\alpha_1,\alpha_2;u_1,u_2)\,p\\
\varepsilon_1\alpha_1' &= \alpha_1\partial_{\alpha_1}\tilde{\mathcal{E}}(\alpha_1,\alpha_2;u_1,u_2)\\
\varepsilon_2\alpha_2' &= \alpha_2\partial_{\alpha_2}\tilde{\mathcal{E}}(\alpha_1,\alpha_2;u_1,u_2)\\
\tilde{\mathcal{E}}_{+,1}(\alpha_1,\alpha_2;u_1,u_2) &= \frac{\alpha_1u_1(1+\alpha_2u_2(1-B))}{(1+\alpha_2u_2)(1+\alpha_1u_1)},\\
\tilde{\mathcal{E}}_{+,2}(\alpha_1,\alpha_2;u_1,u_2) &= \frac{\alpha_2u_2}{1+\alpha_2u_2}\\
\tilde{\mathcal{E}}(\alpha_1,\alpha_2;u_1,u_2,u_2) &= \mathcal{E}_{+,1}(\alpha_1,\alpha_2;u_1,u_2)\\
&\quad - e_1(\alpha_1-\alpha_1^0)_+\theta\big[(1-e_3)\tilde{\mathcal{E}}_{+,2}(\alpha_1,\alpha_2;u_1,u_2) - e_2(\alpha_2-\alpha_2^0)_+\big]
\end{aligned} \tag{31}$$

Though the new model equations are more handy, one effect is scaled away: In the non-scaled equation, presence of substrate u_2 leads to the presence of U_2, and this in turn forces the $\partial_{\alpha_1}\mathcal{E}(\alpha_1,\alpha_2;u_1,u_2)$ to become positive, even if $u_1=0$. This is, substrate two will increase the velocity at which pathway one is activated, even if substrate two is largely hindered to be degraded. In order to re-introduce this effect that has been scaled away, we introduce artificially an interaction term into the net energy $\tilde{\mathcal{E}}(\alpha_1,\alpha_2;u_1,u_2)$, but leave the energy gain functions $\tilde{\mathcal{E}}_{+,1}$ and $\tilde{\mathcal{E}}_{+,2}$ unchanged. We define

$$\hat{\mathcal{E}}(\alpha_1,\alpha_2;u_1,u_2,u_2) = \tilde{\mathcal{E}}(\alpha_1,\alpha_2;u_1,u_2,u_2) + \psi\frac{\alpha_1u_2}{1+\alpha_1u_2}. \tag{32}$$

That is, in presence of u_2, the energy $\tilde{E}$ increases in α_1. This fact forces pathway one to increase its potential activity if substrate u_2 is present. Please note that, for $\alpha_1=u_1=0$, we obtain the overall form of a single substrate pathway for u_2, and for $u_2=\alpha_2=0$, we have for substrate u_1 the usual single-pathway model. The model here is a direct generalization of single-pathway dynamics to a hierarchical topology of substrate processing networks.

4. Application to data

4.1. Batch experiments

We consider the degradation of toluene, acetate and benzoate by *G. metallireducens*. In the present section, we focus on four batch experiments: two experiments where acetate and benzoate are offered alone, and two experiments with two substrates present at the same time: toluene and acetate, resp. toluene and benzoate [25,26].

In *G. metallireducens*, the important stepping stones in the metabolism are the conversion of toluene and benzoate to benzoyl-CoA [33,2], resp. the conversion of benzoyl-CoA and acetate to acetyl-CoA [2,47]; acetyl-CoA is a central intermediate product of a class of substrates that enters the TCA cycle, one central

energy-producing pathway. Among other things, the energy produced here is used to produce biomass or energy [14] (see Fig. 6).

There is, of course, some degree of freedom in the interpretation of the metabolism; in particular which step is to consider as "bottleneck" has some arbitrary aspects. We know that benzoate and benzoyl-CoA are rather similar, and only minimal reactions are required to transform benzoate into benzoyl-CoA. Though toluene is also rather readily transformed into benzoyl-CoA, at least two intermediate steps are necessary. We thus assume that these two substances form a hierarchical pathway. The intermediate product, benzoyl-CoA, as well as acetate are both converted into acetyl-CoA, which in turn is – via the TCA cycle – eventually also converted into biomass. There are several reactions necessary for the transformation of benzoyl-CoA into acetyl-CoA, while only one step is required to transform acetate into acetyl-CoA. However, we simplify the situation in considering benzoyl-CoA and acetyl-CoA as close relatives, and grouping them together as one entry node into the TCA cycle. We thus only place a bottleneck downstream of acetyl-CoA, and consider the pathway from acetate resp. benzoate-CoA as early converging.

Following this line of reasoning, we set up one single model for the pathway and all experiments. Only initial conditions of the concentrations in toluene, benzoate and acetate are adapted in order to reproduce the data of four batch culture experiments: acetate only, benzoate only, acetate and toluene, and benzoate and toluene. p denotes the population size, and acetate, benz, tol denote the concentrations of acetate, benzoate and toluene, and α_a, α_b and α_t the respective activity variables. In addition, also FeII has been measured in the experiment; as *G. metallireducens* is anaerobic microorganism it uses FeIII as electron acceptor and during degradation of carbon sources the FeIII is reduced into FeII which can be monitored. FeII is generated in the degradation of all three substances, and is thus an additional indicator about the amount of substrate consumed. Although sometimes a large variance in the FeII data can be observed, it can be used as an additional, advantageous check of the system and model.

In order to build up the model, we define the energy gain and the loss for the different pathways, and describe how to combine the energies to the complete model. First of all, the concentrations of acetate, benzoate and toluene that are to process (modulated by the activity variables) read

$$\alpha_a\,\text{acetate}, \quad \alpha_b\,\text{benz}, \quad \alpha_t\,\text{tol}.$$

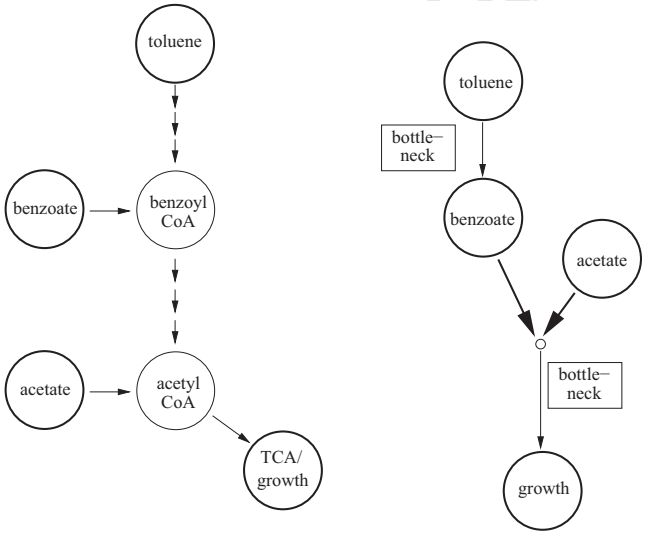

Fig. 6. Structure of toluene, benzoate, and acetate pathway. Left panel: biochemistry, right panel: model approach. Bold circles appear in our model.

We first consider the fate of toluene: toluene is pre-processed to benzoyl-CoA. Let T denote the intermediate product that is fed into the benzoate pathway. We have the equation for the dynamics of T given by

$$\varepsilon_T T' = \hat{B}_t \frac{\alpha_t \text{tol}}{1+\alpha_t \text{tol}} - \check{B}_2 \mathcal{E}_{t,+}. \tag{33}$$

Connected with this pre-processing are not only the costs for the potential activity of the pathway $e_t(\alpha_t - \alpha_t^0)_+$, but also costs per processed toluene molecule, i.e. the energy required to process tol is proportional to $\alpha_t\text{tol}/(1+\alpha_t\text{tol})$. Three substrates at different concentrations are fed into the Michaelis–Menten processing device downstream the convergence point: $\alpha_b T$, $\alpha_b$benz, and $\alpha_a$acetate. From that, we are able to define the different contributions to the overall energy:

$$\begin{aligned}
\text{gain(acetate)}\ \mathcal{E}_{a,+} &= \alpha_a \text{acetate}/(1+\alpha_a \text{acetate} \\
&\quad + \alpha_b \text{benz} + \alpha_b T) \\
\text{costs(acetate)}\ \mathcal{E}_{a,-} &= e_a(\alpha_a - \alpha_a^0)_+ \\
\text{gain(benz.)}\ \mathcal{E}_{b,+} &= \alpha_b \text{benz}/(1+\alpha_a \text{acetate} + \alpha_b \text{benz} + \alpha_b T) \\
\text{costs(benz.)}\ \mathcal{E}_{b,-} &= e_b(\alpha_b - \alpha_b^0)_+ \\
\text{gain(pre-pr.tol.)}\ \mathcal{E}_{t,+} &= \alpha_b T/(1+\alpha_a \text{acetate} + \alpha_b \text{benz} + \alpha_b T) \\
\text{costs(pre-pr.tol.)}\ \mathcal{E}_{t,1,-} &= e_t(\alpha_t - \alpha_t^0)_+ \\
\text{loss(pre-processing)}\ \mathcal{E}_{t,2,-} &= \alpha_t \text{tol}/(1+\alpha_t \text{tol})
\end{aligned}$$

An overall maintenance energy of the metabolism is neglected, as this energy is known to be extremely low in case of *G. metallireducens* [21]. We follow the reasoning in Section 3 (hierarchical model): we let $\varepsilon_T \to 0$, and introduce additionally an interaction term between toluene and benzoate,

$$\mathcal{E}_{TB} = \alpha_b \text{tol}/(1+\alpha_b \text{tol}). \tag{34}$$

The experimental results indicate that the acetate pathway is (indirectly) activated by toluene (compare the time scale for acetate degradation in Figs. 7 and 10). The biochemistry of *G. metallireducens* supports this conjecture up to a certain degree, since toluene is degraded via benzoyl-CoA into acetyl-CoA; to mimic this process, we additionally introduce the interaction energy

$$\mathcal{E}_{TA} = \alpha_a \text{tol}/(1+\alpha_a \text{tol}). \tag{35}$$

Note that these terms do not appear directly in the consumption of nutrients or biomass production, but that these terms influence the control variables. The interaction terms formulate additional aspects of the pathway that controls the nutrient uptake, and not the uptake itself. Details of the model can be found in Appendix C.

We fit this model simultaneously to four batch experiments with acetate only, benzoate only, and the combinations of acetate/toluene resp. benzoate/toluene. Note that not all components have been measured in all experiments; however, there is sufficient information to adapt the model in a sensible way. The rate constants of the model are the same for all experiments, only the initial conditions are adapted. The parameters are stated in Appendix C, the simulation and data are shown in Figs. 7–10.

The first point to note is that the model structure represents the biochemical pathways well enough to allow not only for qualitative but also for quantitative analysis of the data. If we consider the data and model results more in detail, we find that benzoate and toluene are processed at the same time (Fig. 9, corresponding to regions D_1, D_2 and E in Fig. 5). Furthermore, as expected on basis of the topology and our theoretical considerations, we find that acetate inhibits toluene consumption (Fig. 10, region C_2 in Fig. 3): the classical diauxic growth can be observed in Fig. 10. Additionally, we nicely observe the effect of cross-linking between

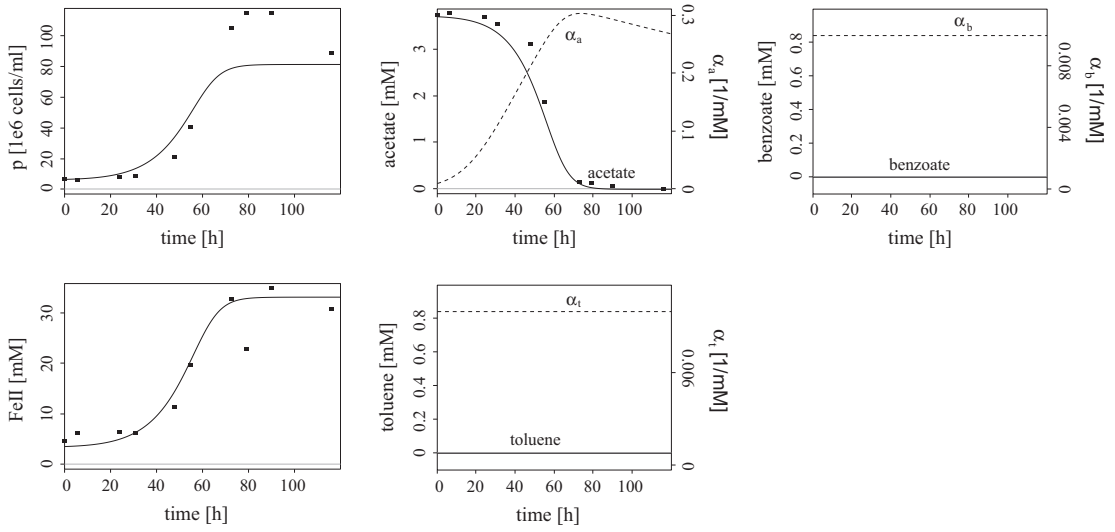

Fig. 7. Batch experiment: acetate only (data: dots, curves: result of the model).

the pathways. If only acetate resp. benzoate is present, the control variables of the other two pathways stay at the basal level. Toluene, however, activates via the interaction terms the acetate as well as the benzoate pathway. In presence of toluene, α_A and α_B are increased also if no acetate resp. benzoate is present (Figs. 9 and 10). The activation of the benzoate pathway by toluene is natural as benzoate (better: benzoyl-CoA) is an intermediate product of the toluene pathway, and since benzoyl-CoA is processed into acetyl-CoA one can understand why also the acetate pathway is activated.

We may infer from the model the interaction characteristics of acetate and benzoate (though this substrate combination is not directly investigated in the batch experiments). If we use the parameter values determined, and assume a fixed acetate resp. benzoate concentration, Fig. 11 indicates the optimal nutrient consumption strategies. If the acetate concentration is predominating, acetate will hinder benzoate to be consumed. Only if very few acetate but a high benzoate concentrations are present, the bacteria will prefer benzoate over acetate. Of special interest is a substantial region of combinations of concentrations (gray shaded), where the degradation of benzoate only resp. the degradation of acetate only form local maxima. While the single cell should concentrate on one nutrient only, the population may decide for one nutrient only, or to consume both nutrients in parallel. It is not clear if the nutrient uptake strategy will be homogeneous or heterogeneous in the population, i.e. if all cells decide for the same strategy, or if the population splits in two phenotypes, each of them specialized to one nutrient. Even oscillatory behavior cannot be excluded, where individuals or the population switches periodically or randomly between feeding first on one and then on the other substrate.

4.2. Retentostat

In order to further validate the model approach, we analyzed three further experiments using the retentostat, and acetate/benzoate as substrate combination. A retentostat is a device similar to a chemostat, in which the bacteria are not washed out but are kept in the reaction vessel. The ecological situation and the physiology of bacteria under retentostat conditions relatively to batch is very different [25,26]. It is not clear at all, if a model, adapted to batch culture experiments, can be adapted to a

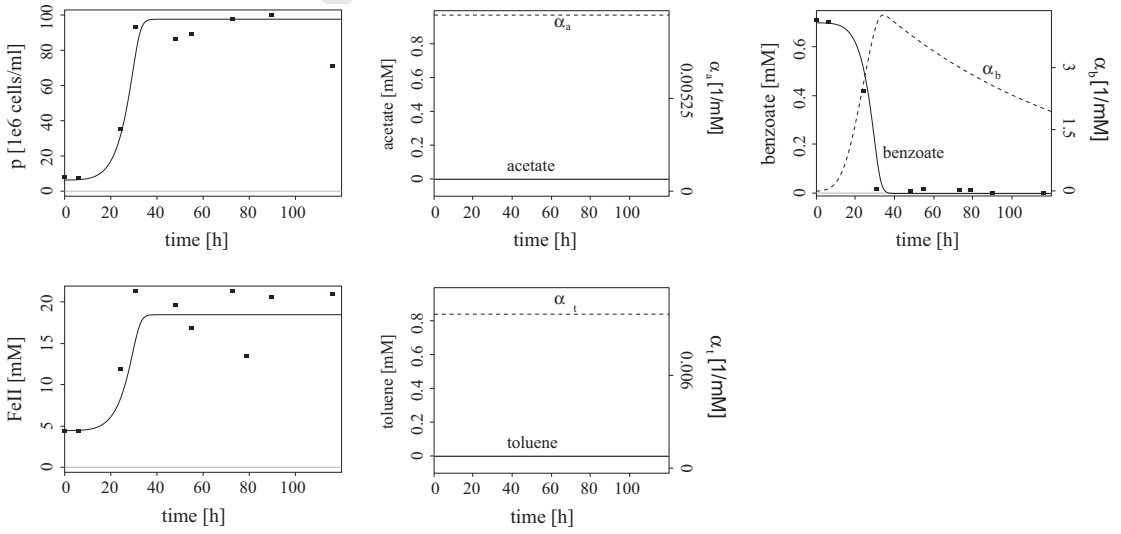

Fig. 8. Batch experiment: benzoate only (data: dots, curves: result of the model).

Q1 Please cite this article in press as: J. Müller et al., Model selection for microbial nutrient uptake using a cost-benefit approach, Math. Biosci. (2014), http://dx.doi.org/10.1016/j.mbs.2014.06.012

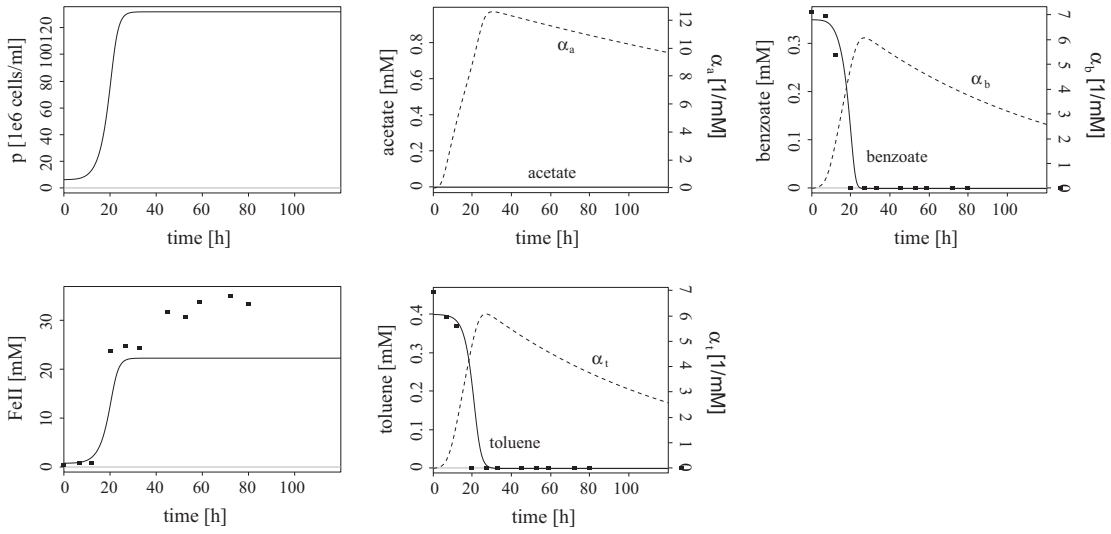

Fig. 9. Batch experiment: benzoate and toluene (data: dots, curves: result of the model).

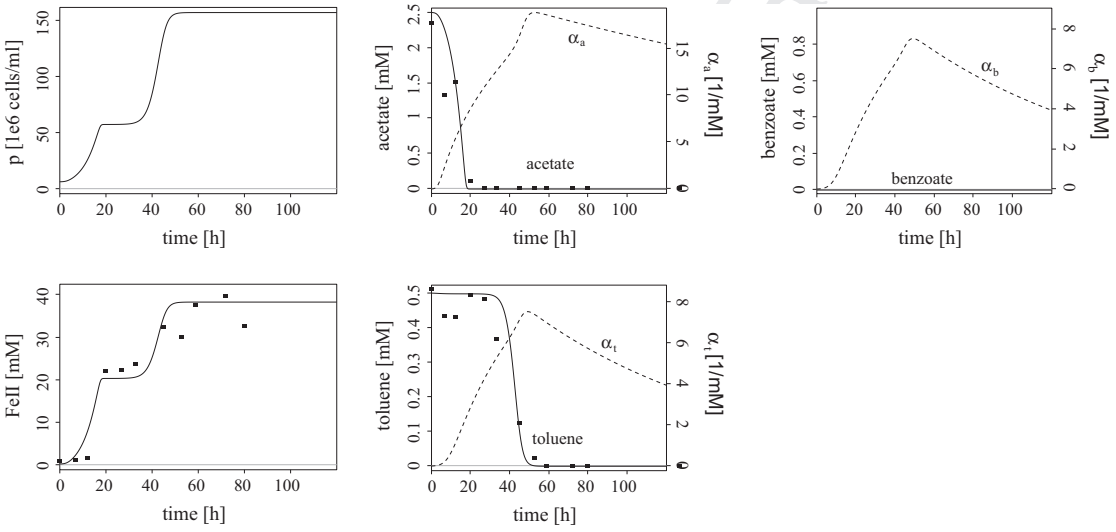

Fig. 10. Batch experiment: acetate and toluene (data: dots, curves: result of the model).

retentostat. A second challenge for the model is the fact, that this substrate combination (acetate/benzoate) has not been present in the batch culture experiments, s.t. the model has only been able to indirectly learn what to expect in this situation.

The adaptation of the model structure is straight, only inflow and outflow has to be added where necessary (see Appendix C). The flow rates are known. We used the rate constants obtained by the batch culture up to one rate: the growth rate of bacteria due to acetate, A_a, had to be adapted; and, of course, initial conditions required adaptation. With these little modifications, the model is able to explain the data quite well for the first and the third replicate for the first 120 h (see Figs. 12 and 14). In these two replicates, we basically find catabolite repression as expected from the analysis of the toluene/acetate batch culture experiments. In the second replicates, acetate seems to oscillate (Fig. 13). In this case, the overall concentration range is met by the model, but the model does not follow the time course of the data in detail. We excluded the time after 120 h in our analysis, as the cells started to attach to the vessel wall and seemed to initiate biofilm formation. From this time on, the behavior is not comparable any more with the batch experiments.

If we compare the data of the three replicates, we find the second replicate differs strongly from the first and the third, quantitatively as well as qualitatively. The reason for this is by no means clear. A possible explanation is offered by Fig. 11: the acetate/benzoate concentration measured in the retentostat are close or within the bistable region indicated in Fig. 11. It may happen that cells switch between the different behavioral pattern (consumption of benzoate resp. consumption of acetate) in a complex manner. Depending on initial conditions, a heterogeneous population may lead to the complex, dynamical patterns observed in the experiments. In particular, it is possible that the oscillatory behavior as observed in the second replicate is a consequence of the adaptation of the abundance of phenotypical subtypes. However, there are other and more explanations possible.

5. Discussion

Our study aims to deepen the understanding of driving forces behind the interactions of metabolic pathways. It can help to predict the degradation dynamics e.g. in bioremedation processes, if some core properties of the involved catabolic pathways are

Q1 Please cite this article in press as: J. Müller et al., Model selection for microbial nutrient uptake using a cost-benefit approach, Math. Biosci. (2014), http://dx.doi.org/10.1016/j.mbs.2014.06.012

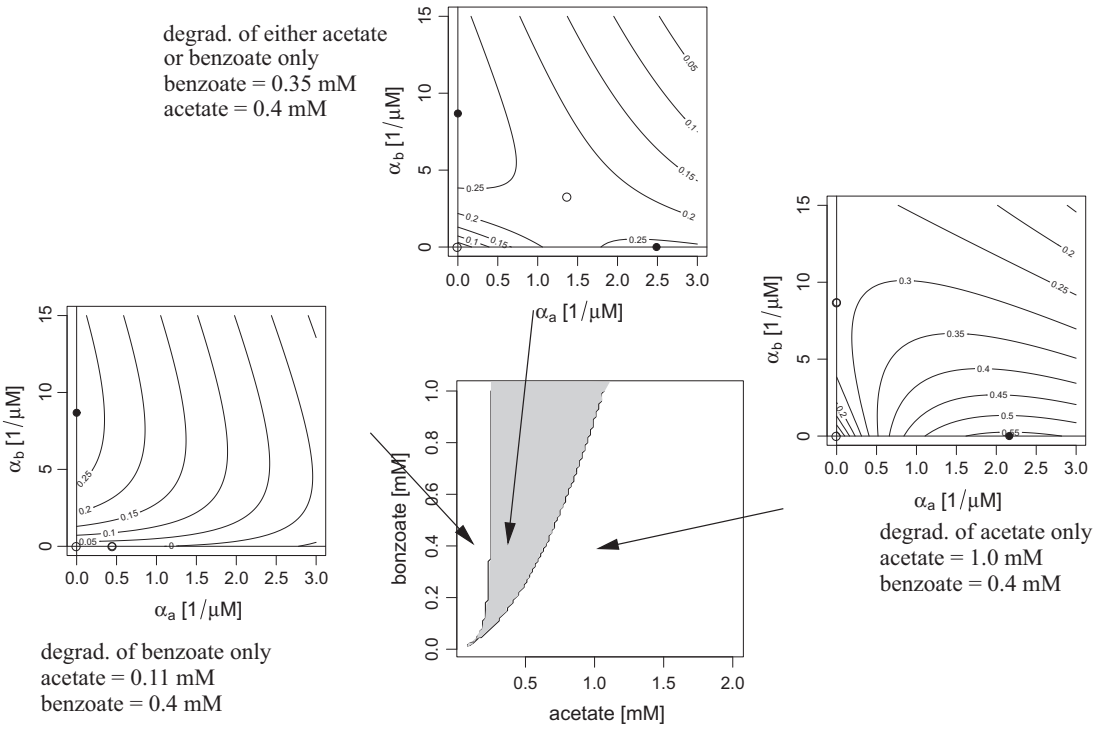

Fig. 11. Bifurcation analysis in presence of fixed acetate/benzoate concentration (central figure). The gray shaded region indicates the bistable domain. The peripheral figures show a contour plot of the net energy over α_a, α_b for given values of the concentrations (indicated by the arrows); local maxima are indicated by bullets, extremal points that fail to be local maxima by open circles.

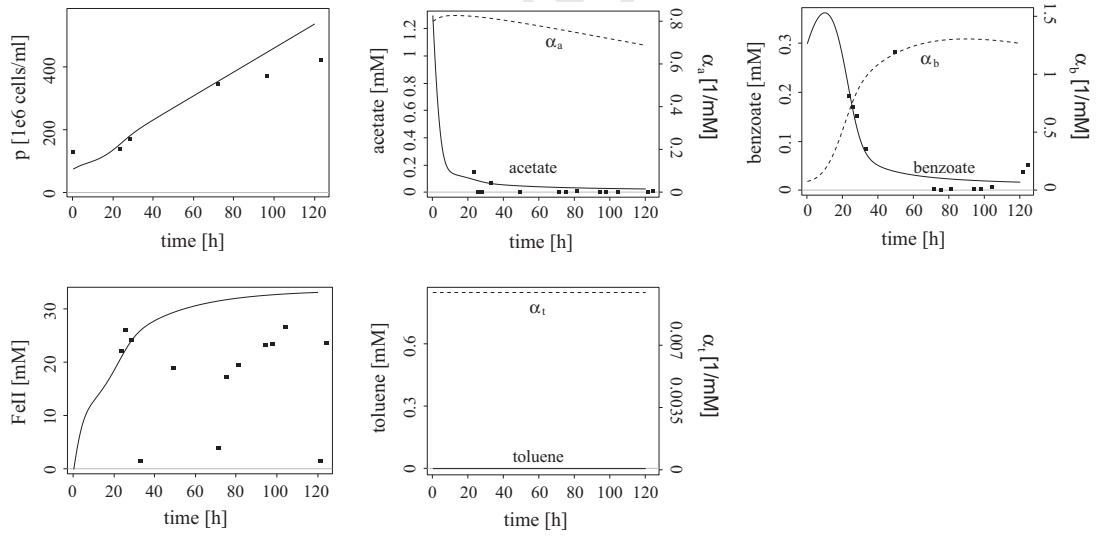

Fig. 12. First replicate of the retentostat (“retent. 1”). Dots: data, curves: result of the model.

known. Vice versa, in cases of unknown catabolic pathways, observed degradation dynamics for different substrates give hints about the underlying topology. The approach is based on the idea that a cell tries to optimize its energy intake. It is necessary to note that an implicit assumption underlying all these considerations is that evolution forced the cells to optimize the pathways indeed. If the possible advantage is too small, this optimization may not take place. Furthermore, it may be that the cells are still in a transient stage, and the optimization is still not complete. In such situations, the results discussed here are not applicable. However, this approach is for example close to metabolic control theory due to Kascar et al. [16] and cybernetic modeling of metabolic fluxes [20,41,34]. Kascar still requires a fundamental knowledge of fluxes within the cell. This is far more than what we want to ask as prerequisite for modeling. The differences to cybernetic models are mainly the treatment of costs connected to the activity of a pathway; we propose to introduce a generic term explicitly addressing the burden, while mostly cybernetic addresses these costs not explicitly, but by an appropriate formulation of the metabolic chain, including the production of enzymes required to activate the pathway. The simplicity of the present approach allows to formulate models with less knowledge about the metabolic chains,

Q1 Please cite this article in press as: J. Müller et al., Model selection for microbial nutrient uptake using a cost-benefit approach, Math. Biosci. (2014), http://dx.doi.org/10.1016/j.mbs.2014.06.012

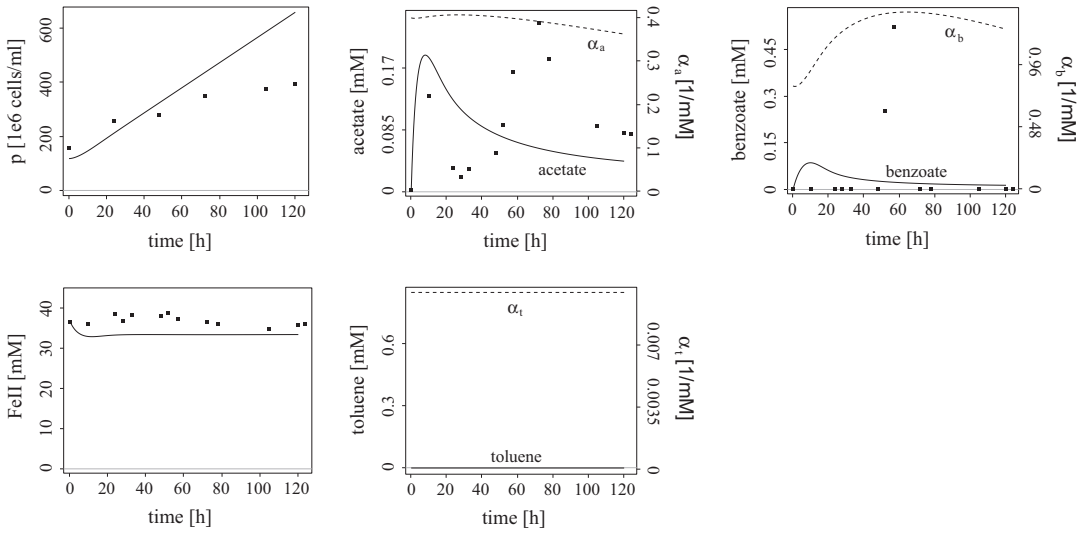

Fig. 13. Second replicate of the retentostat ("retent. 2"). Dots: data, curves: result of the model.

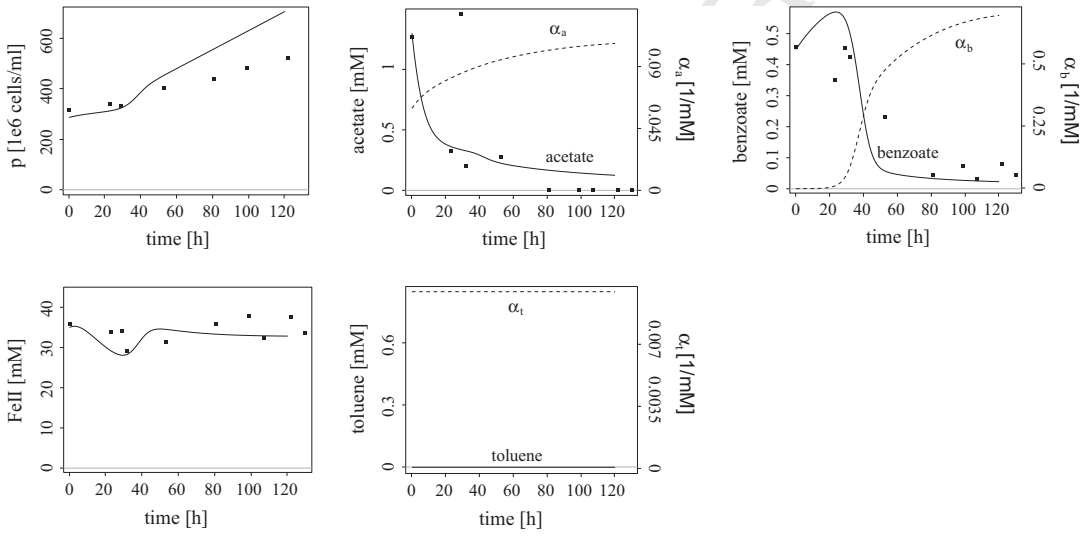

Fig. 14. Third replicate of the retentostat ("retent. 3"). Dots: data, curves: result of the model.

as we use Monod terms and linear functions, implicitly claiming that these functions are generically sufficient approximations of more complex, "true" functional responses. We developed this idea, following two different lines of reasoning: a qualitative, theoretical analysis allowed to classify different consumption strategies; a quantitative application to data validating the concept and allowing to investigate batch- and retentostat experiments.

The theoretical considerations identified situations where different behavior is to expect. The results indicate that the overall topology of the pathway is decisive. In the present work, we distinguish three, basic topologies: two independent pathways (parallel topology), two pathways competing for one enzymes (early converging topology), and the case that one substrate is intermediately converted into the other substrate (hierarchical pathway). The first possibility leads to a simultaneous degradation of the substrates. Early converging as well as hierarchical topologies have catabolite repression as consequence: if the concentration of substrate one is much higher than that of substrate two (in the sense that it pays considerably more to degrade substrate one), the consumption of substrate two is repressed. It is to note that this repression is basically symmetric: also the substrate two may repress substrate one if the concentrations are in favor for it. However, it may happen that this reversed situation appears only if substrate one is present in extremely low concentrations. If we change the concentrations, somewhere a transition between the repression of the first substrate by the second, and the second by the first appears. It is this transition, where the early convergent and the hierarchical pathways are different. In the case of early convergent pathways, a bistable region appears. Within this region, the consumption strategy "consume only one substrate" forms a local optimum, for consumption of substrate one as well as for consumption of substrate two. Though one of the local optima is most likely slightly better than the other, we nevertheless expect a region where the two local optima are *de facto* equivalent. From the present analysis it is not clear what the population will do – split into two phenotypes, or decide to go for one substrate only. Inspired by optimization theory, we expect the population to split into two sub-populations, each of them targeted on one substrate. The hierarchical pathway shows even a richer dynamic: depending on the parameters and on the concentrations, either a bistable region with two one-substrate-only solutions, a bistable region with one both-substrates and one one-substrate-only strategy, or

Q1 Please cite this article in press as: J. Müller et al., Model selection for microbial nutrient uptake using a cost-benefit approach, Math. Biosci. (2014), http://dx.doi.org/10.1016/j.mbs.2014.06.012

a region with parallel consumption of both substrates by all cells appear.

All in all, we have three basic carbon utilization pattern: parallel consumption, catabolite repression, and a bistable behavior, where individual cells only access one carbon source, but the population (may) split into two phenotypical subtypes, s.t. on population level both carbon sources are utilized. Schreiber and Tobiason [36] consider an ecological model for allocation strategies in case of two resources. They distinguish between antagonistic, substitutable, complementary and essential resources. In case of substitutable resources they predict that the allocation strategy is a random distribution over the resources. However, the authors conclude that this situation is highly unstable as any modification of the model that introduce some aspect of antagonism leads to the formation of specialized sub-populations. The difference between the present and that model is in particular the formulation of costs related with the allocation of a resources. In [36], costs are only taken into account in so far as the total uptake rate is limited, and can be distributed between the two resources. Therefore it is not strictly possible to connect different topologies in the present work to different resource types in their work. It is perhaps possible to relate the parallel topology to the substitutable case. In case of early converging or hierarchical structure, our model can be considered as antagonistic: the uptake of one resource decreases the uptake rate of the other resource in a nonlinear fashion. In this interpretation, our conjecture that this competition of substrates in the processing chain leads to heterogeneity in the population is in line with the conclusions in [36].

It is remarkable that – in contrast to parallel consumption and catabolite repression – almost no heterogeneous utilization strategies, i.e. formation of two specialized microbial sub-populations, are reported. At least, heterogeneous uptake of leucine by *Cytophaga-Flavobacter* has been found [39]. Even more interesting is the discussion in [18]. This paper studies the simultaneous uptake of pentose and hexose sugars; very often catabolite repression hinders the simultaneous consumption. There are, however, microbial species or strains, where the different sugars are utilized in parallel. It is not clear, if single cells access both carbon sources, or if the cells specialize. In a second study [19] the authors found differences between cells of the species *Lactobacillus brevis* in their uptake behavior, depending on the history of the cells. Recent results indicate heterogeneity in the TOL system ([30] and references herein); the TOL system degrades toluene in two steps: first it is degraded to benzoate/3-methylbenzoate, which in turn can be easily converted into intermediates for the central metabolism. Seemingly, in particular the first step is only done by a sub-population; the diffusing benzoate/3-methylbenzoate can be then consumed by all of the bacteria. Also this is an example for heterogeneity in nutrient uptake, this time in case of a single nutrient. The reason that heterogeneous uptake strategies are seldom monitored could be also caused by the fact that this behavioral type is difficult to recognize, and does not necessarily indicate that it is not abundant.

In order to validate this approach, and to test if not only qualitative but also quantitative conclusions are possible by means of this structure, we modeled the degradation of acetate, benzoate and toluene by *G. metallireducens*. We first applied the model to four batch experiments. A large simulation model for the metabolism of *G. metallireducens* is described in [42]. The starting point of that model is the genome of the bacteria, comparison with similar bacteria and flux balance analysis. Though it represents a useful tool, it is difficult to validate these large simulation models and to extract reliable information. Our approach is at the other end of the complexity, taking into account only very little pre-knowledge about the topology of the pathways. Therewith it was possible to explain all four experiments by means of one single model, without e.g. changing the rate constants. In particular, we found in accordance with the theory catabolic repression of toluene by acetate. The combination of benzoate and acetate has not been addressed in the batch culture experiments, but the theory predicts also here catabolic repression resp. bistable situations. Next, we extended the model describing batch culture to retentostat experiments with benzoate and acetate. Even here, only minor adaptations (concerning one rate constant only) have been necessary to explain the data for two of the three replicates; though rather different in detail, these two replicates showed catabolic repression as predicted before. The third replicate showed oscillatory behavior – the model has only been able to meet the overall range for the concentration but not to follow the precise time course. An explanation (which is only one explanation possible, but an interesting one) is, that the concentrations met the bistable region. That is, heterogeneity and complex switching between the two optimal consumption strategies may lead to rather heterogeneous experimental results.

Naively, one would expect that the pathways consisting of many, tightly controlled, and sophisticated biochemical reactions, cannot be covered by the model developed by rather qualitative considerations. However, also many models that describe chemostat or batch culture use e.g. Monod- or Hill functions to describe substrate uptake, are able to quantitatively reproduce and predict data. Our approach is a direct generalization of these models, taking into account possible interactions between different pathways. On that basis, we expect that the present finding, the ability to reproduce and predict experimental data in a quantitative way, is not a coincidence but is a generic property of the modeling approach.

Although the constraints are not too tight, the model naturally does not cover all possible scenarios. In particular, there are three shortcomings: (1) the core idea of the model does not cover spatio-temporal heterogeneities, (2) the model approach focuses on single cells, and not on the population and (3) the model does not take into account interaction with different microbial species or other organisms as plants and higher animals.

Spatio-temporal heterogeneities may lead to more complex strategies. It is possible that a typical time-pattern of appearance and disappearance of substrates forces cells to keep pathways potentially active, even in absence of the substrate, in order to allow for a fast degradation.

To focus on the population instead of single cells is necessary as some situations are not to decide on single cell level. An example are the bistable uptake pattern revealed in the analysis. Another example is bet hedging [5,29]: a small fraction of the population selects a suboptimal state in order to survive or grow fast if the environment changes.

Further interesting aspects not yet included in the actual state of our model arise from the growing field of sociomicrobiology [31], which understands bacterial populations as social entities. This allows to safe maintenance costs for e.g. extracellular activities as pre-processing of large substrate molecules. This might be organized in a cell density, or more generally, efficiency depending way [10,13]. Interestingly, almost all quorum sensing systems control extracellular degrading enzymes. Our cellular model, which does not consider the population, predicts that for the hierarchical pathways under certain conditions it can be optimal for cells to degrade any of the substrate, but not both simultaneously. This hints to the possibility of a controlled differentiation of isogenic bacteria populations, allowing division of work which optimizes colony growth and survival (see e.g. [22]). Other abiotic and biotic factors also interact with optimization of catabolic processes. Examples comprise cross feeding with other species, concentration of other potentially relevant, e.g. limiting factors, which might even be affected by the catabolic process itself (e.g. electron

Q1 Please cite this article in press as: J. Müller et al., Model selection for microbial nutrient uptake using a cost-benefit approach, Math. Biosci. (2014), http://dx.doi.org/10.1016/j.mbs.2014.06.012

acceptors), the existence of more than one catabolic pathway for a substrate in a cell, and a dependency of the net energy gain on environmental or physiological conditions. Under some conditions, for example in the presence of a high competitive pressure by other species, a faster, but with respect to net energy gain more inefficient catabolic pathway may benefit the overall performance of a population [9].

Appendix A. Analysis of two early converging pathways

The derivatives of the net gain w.r.t. α_1 (α_2) read

$$\partial_{\alpha_1}\mathcal{E} = \frac{u_1(1+(1-\theta)\,\alpha_2 u_2)}{(1+\alpha_1 u_1+\alpha_2 u_2)^2} - e_1$$

$$\partial_{\alpha_2}\mathcal{E} = \theta\left(\frac{u_2(1+(1-1/\theta)\,\alpha_1 u_1)}{(1+\alpha_1 u_1+\alpha_2 u_2)^2} - e_2\right).$$

There are natural candidates for the control: the single-substrate strategies $(\alpha_1,\alpha_2) = (\alpha_1^*, 0)$ resp. $= (0,\alpha_2^*)$. We know the solution for a single substrate:

$$\alpha_i^* u_i = (\sqrt{u_1/e_i} - 1)_+.$$

Is $(\alpha_1^*, 0)$ a local minimum or maximum? We are inspecting the sign of $\partial_{\alpha_2}\mathcal{E}$ at $(\alpha_1^*, 0)$. We identify the curve $\partial_{\alpha_2}\mathcal{E} = 0$, at which the strategy switches from local maximum to saddle point,

$$\begin{aligned} 0 = \partial_{\alpha_2}\mathcal{E}|_{\alpha_1^*,0)} &= \theta\left(\frac{u_2(1+(1-1/\theta)\,\alpha_1 u_1)}{(1+\alpha_1 u_1)^2} - e_2\right) \\ &= \theta\left(\frac{u_2(1+(1-1/\theta)\,(\sqrt{u_1/e_i}-1)_+)}{(1+(\sqrt{u_1/e_i}-1)_+)^2} - e_2\right) \;\Rightarrow\; (u_2/e_2) \\ &= \frac{(1+(\sqrt{u_1/e_i}-1)_+)^2}{(1+(1-1/\theta)\,(\sqrt{u_1/e_i}-1)_+)}. \end{aligned}$$

For $u_1 < e_1$ this curve becomes trivial (u_2 equals e_2 in this case); let us assume that $u_1 > e_1$. Then, $(u_2/e_2) = f(u_1/e_1;\theta)$ with

$$f(x) = \frac{x}{1/\theta + (1-1/\theta)\,\sqrt{x}}.$$

In a similar way, the control $(\alpha_1,\alpha_2) = (0,\alpha_2^*)$ can be investigated; we find, that in this case the stability changes at

$$(u_1/e_1) = f(u_2/e_2; 1/\theta)$$

with the same function $f(x)$ as defined above; this finding can be obtained by the following observation: if we exchange substrate one and substrate two (renaming the corresponding variables), then θ is transformed into $1/\theta$. As the properties of the energy function (local maxima and minima) are not changed by renaming the variables, we have an invariance of the system under the transformation $(u_1,\alpha_1,u_2,\alpha_2,\theta) \mapsto (u_2,\alpha_2,u_1,\alpha_1,1/\theta)$. We note that $f(x;1) = x$. I.e., for $\theta = 1$ the two curves coincide.

Definition. Let $y_a(x) = \sqrt{f(x^2,\theta)}$, where $x \in \mathbb{R}_+$ if $\theta \geqslant 1$, and $x \in [0,(1-\theta)^{-1})$ in case of $\theta \in (0,1)$. $y_b(x)$ is defined by $x^2 = f(y_b^2; 1/\theta), y_b \geqslant 0$.

Bifurcations happen at the curves $u_1/e_1 = y_a(u_2/e_2)$, and $u_1/e_1 = y_b(u_2/e_2)$.

Proposition. *If $\theta \neq 1$, $\theta > 0$, $y_a(x) = y_b(x)$ happens only for $x = 0$, $y_a(0) = y_b(0) = 1$, and $x = 1$, $y_a(1) = y_b(1) = 1$.*

Proof. For $x = 0$, we find $y_a(0) = y_b(0) = 0$;. Now assume that $x \neq 0$. If $y_a(x) = y_b(x) = y$, we find

$$x^2 = \frac{\frac{x^2}{\theta^{-1}+(1-\theta^{-1})x}}{\theta+(1-\theta)y} \Rightarrow y = \frac{1}{1-\theta}\left(\frac{\theta}{1+(\theta-1)x} - \theta\right) = \frac{x}{\theta^{-1}+(1-\theta^{-1})x}.$$

Hence,

$$\frac{x^2}{\theta^{-1}+(1-\theta^{-1})x} = y^2 = \left(\frac{x}{\theta^{-1}+(1-\theta^{-1})x}\right)^2 \Rightarrow \theta^{-1}+(1-\theta^{-1})x = 1.$$

This in turn, implies $x = 1$ and $y = 1$. □

Proposition. *Let $\theta \in \mathbb{R}_+ \setminus \{1\}$. Then,*

$$y_a(x) > y_b(x) \quad \text{for } x > 1$$

if $y_a(x)$ is defined.

Proof. We first show that $y_a'(1) > y_b'(1)$. Thereto we note that

$$\begin{aligned} \frac{d}{dx}f(x^2;\theta) &= \frac{2x(\theta^{-1}+(1-\theta^{-1})x) - x^2(1-\theta^{-1})}{(\theta^{-1}+(1-\theta^{-1})x)^2} \\ &= \frac{2x\theta^{-1}+(1-\theta^{-1})x^2}{(\theta^{-1}+(1-\theta^{-1})x)^2}. \end{aligned}$$

Thus,

$$y_a'(1) = \left.\frac{\frac{d}{dx}f(x^2;\theta)}{2\sqrt{f(x^2;\theta))}}\right|_{x=1} = (1+\theta^{-1})/2.$$

From $1 = (d/dx)\sqrt{f(y_b(x)^2;1/\theta)}$, we conclude that

$$1 = y_b'(x)\left.\frac{\frac{d}{dy}f(y^2;1/\theta)}{2\sqrt{f(y^2;1/\theta))}}\right|_{x=1,y=1} \Rightarrow\; y_b(1) = \frac{2}{1+\theta}.$$

The inequality $y_a(1) > y_b(1)$ is equivalent with $\theta + 2 + 1/\theta > 4$. The minimum of $\theta + 1/\theta$ is located at $\theta = 1$; thus, for $\theta \geqslant 0,\ \theta \neq 1$, we indeed find $0.5(1+1/\theta) > 2/(1+\theta)$.

Above we showed that $y_a(x)$ and $y_b(x)$ do not intersect for $x > 1$. Therefore, from $y_a(1) = y_b(1)$, and $y_a'(1) > y_b'(1)$, we conclude $y_a(x) > y_b(x)$ for $x > 1$. □

In the region $\Omega_1 := \{(x,y)|y_a(x) > y > 1, x > 1\}$, the function $\mathcal{E}(u_1,\alpha_1,u_2,\alpha_2)|_{u_1=xe_1,u_2=ye_2}$ possesses a local maximum on the axis $\{\alpha_2 = 0\}$; in $\Omega_2 := \{(x,y)|y > \max\{y_a(x),1\},\ x > 1\}$, a local maximum is on the axis $\{\alpha_1 = 0\}$. Numerical analysis shows that for $(u_1/e_1, u_2/e_2) \in \Omega_1 \cap \Omega_3$, there are two maxima on the axis, and a saddle point in the interior of the positive cone.

Appendix B. Analysis of two hierarchical pathways

We consider the static situation for two hierarchical pathways as stated in Section 2.2.3. We are interested at extremal points (especially: maxima) of the energy function for $\alpha_1\alpha_2 > 0$. As the energy function is zero for $\alpha_1 = \alpha_2 = 0$, and becomes negative if either α_1 or α_2 is larger than a certain, positive constant, we may restrict ourselves to a compact region of the positive quadrant in order to find all relevant maxima. This is, we already know that we have at least one global maximum; we may have several local maxima.

We expect (for different parameters resp. substrate concentrations) up to four different minima/maxima of the energy function in (α_1,α_2):

$$(0,0), \quad (\alpha_1^*,0), \quad (0,\alpha_2^*), \quad (\alpha_1^{**},\alpha_2^{**})$$

where $\alpha_1^*,\ \alpha_2^*,\ \alpha_1^{**},\ \alpha_2^{**} > 0$.

We will compute these four solutions resp. find conditions s.t. these solutions are local maxima. We will use u_1/e_1 and u_2/e_2

Q1 Please cite this article in press as: J. Müller et al., Model selection for microbial nutrient uptake using a cost-benefit approach, Math. Biosci. (2014), http://dx.doi.org/10.1016/j.mbs.2014.06.012

as bifurcation parameters. At the end, we will find that we need to distinguish $e_3 \in (0, 3/4)$ and $e_3 \in (3/4, 1)$, this is, also e_3 is a bifurcation parameter, unfolding some higher codimension bifurcation (codimension of at least three).

Before we start, for convenience we state the partial derivatives of the energy function $\mathcal{E}(\alpha_1, \alpha_2; u_1, u_2)$ w.r.t α_1 and α_2,

$$\mathcal{E}(\alpha_1,\alpha_2;u_1,u_2) = \frac{\alpha_1 u_1}{(1+\alpha_1 u_1)(1+\alpha_2 u_2)} - e_1\alpha_1 + (1-e_3)\frac{\alpha_2 u_2}{1+\alpha_2 u_2} - e_2\alpha_2$$

$$\frac{\partial}{\partial\alpha_1}\mathcal{E}(\alpha_1,\alpha_2;u_1,u_2) = \frac{u_1}{(1+\alpha_1 u_1)^2(1+\alpha_2 u_2)} - e_1$$

$$\frac{\partial}{\partial\alpha_2}\mathcal{E}(\alpha_1,\alpha_2;u_1,u_2) = \frac{(1-e_3)u_2}{(1+\alpha_2 u_2)^2} - \frac{\alpha_1 u_1 u_2}{(1+\alpha_1 u_1)(1+\alpha_2 u_2)^2} - e_2$$

$(\alpha_1, \alpha_2) = (0, 0)$:

The location $(\alpha_1, \alpha_2) = (0, 0)$ is a local maximum, if the partial derivatives at this point are negative, this is,

$$\frac{u_1}{e_1} < 1 \quad \text{and} \quad \frac{u_2}{e_2} < \frac{1}{e_3 - 1}.$$

In this case there is not enough nutrient of either substrate species, s.t. the utilization does not pay at all.

$(\alpha_1, \alpha_2) = (\alpha_1^*, 0)$:

If $\alpha_2 = 0$, we have a single-substrate pathway, s.t.

$$\alpha_1^* = \frac{1}{u_1}\left(\sqrt{\frac{u_1}{e_1}} - 1\right)$$

if $e_1/u_1 < 1$. We inspect the partial derivative w.r.t. α_2 at $\alpha_1^*, 0)$; this point is a local maximum, if

$$0 > \frac{\partial}{\partial\alpha_2}\mathcal{E}(\alpha_1^*, 0; u_1, u_2) = (1-e_3)u_2 - \frac{u_2\,\alpha_1^* u_1}{1+\alpha_1^* u_1} - e_2.$$

All in all, we have a feasible, local maximum in $(\alpha_1^*, 0)$ iff

$$\frac{u_1}{e_1} > 1, \quad \text{and} \quad \frac{u_2}{e_2} < \frac{\sqrt{\frac{u_1}{e_1}}}{1 - e_3\sqrt{\frac{u_1}{e_1}}}.$$

This is, the region where $(\alpha_1^*, 0)$ is a local maximum is strongly enlarged by the interaction term (the effect of $\alpha_2 u_2$ on the energy gain by substrate one). Let us call the curve

$$\frac{u_2}{e_2} = \frac{\sqrt{\frac{u_1}{e_1}}}{1 - e_3\sqrt{\frac{u_1}{e_1}}}$$

the curve $\mathcal{C}_1$.

$(\alpha_1, \alpha_2) = (0, \alpha_2^*)$: We have again the single pathway solution (slightly modified by the term $1 - e_3$),

$$\alpha_2^* = \frac{1}{u_2}\left(\sqrt{\frac{(1-e_3)u_2}{e_2}} - 1\right)$$

if $e_3 < 1 - e_2/u_2$. The condition for this point to be a local maximum reads

$$0 > \frac{\partial}{\partial\alpha_1}\mathcal{E}(0, \alpha_2^*; u_1, u_2) \iff \frac{u_1}{e_1} > 1 + \alpha_2^* u_2.$$

Thus, the point $(0, \alpha_2^*)$ is a feasible, local maximum iff

$$\frac{u_1}{e_1} < \sqrt{\frac{(1-e_3)u_2}{e_2}} \quad \text{and} \quad \frac{u_2}{e_2} > \frac{1}{e_3 - 1}.$$

We may rewrite the first condition, and find

$$\frac{u_2}{e_2} > \max\left\{1/(1-e_3), (u_1/e_2)^2/(1-e_3)\right\} =: H(u_1/e_1).$$

We call $\{u_2/e_2 = H(u_1/e_1) | u_1/e_1 \geqslant 1\}$ curve $\mathcal{C}_2$.

$(\alpha_1, \alpha_2) = (\alpha_1^{**}, \alpha_2^{**})$:

This situation is more involving to address than the previous cases. We first assume α_2 to be fixed and positive, and compute the optimal α_1 in dependence on α_2 using the condition $\partial_{\alpha_1}\mathcal{E}(\alpha_1, \alpha_2, u_1, u_2) = 0$,

$$0 = \frac{1}{(1+\alpha_2 u_2)}\left[\frac{u_1}{(1+\alpha_1 u_1)} - e_1(1+\alpha_2 u_2)\right]$$

$$\alpha_1 = \alpha_1^{**}(\alpha_2) = \frac{1}{u_1}\left(\sqrt{\frac{u_1}{e_1(1+\alpha_2 u_2)}} - 1\right)$$

together with the condition

$$\frac{u_1}{e_1} > 1 + \alpha_2 u_2$$

to ensure that $\alpha_1^{**}(\alpha_2) > 0$. If we plug $\alpha_1 = \alpha_1^*(\alpha_2)$ into the energy, we find

$$\mathcal{E}(\alpha_1^*(\alpha_2), \alpha_2; u_1, u_2) = \frac{1}{1+\alpha_2 u_2} - 2\sqrt{\frac{e_1}{u_1(1+\alpha_2 u_2)}} - \frac{e_1}{u_1} + (1-e_3) \times \frac{\alpha_2 u_2}{1+\alpha_2 u_2} - e_2\alpha_2.$$

The derivative of this term w.r.t. α_2 is zero for α_2^{**}. We obtain the equation

$$0 = \frac{-u_2}{(1+\alpha_2^{**}u_2)^2} + \sqrt{\frac{e_1}{u_1}}\frac{u_2}{(1+\alpha_2^{**}u_2)^{3/2}} + \frac{(1-e_3)u_2}{(1+\alpha_2^{**}u_2)^2} - e_2.$$

If we multiply this equation by $(1+\alpha_2 u_2)^2/e_2$, we may introduce the functions $g_1(x)$ and $g_2(x)$ to re-write this condition in the following way

$$g_1(x) = -e_3\frac{u_2}{e_2} + \sqrt{\frac{e_1}{u_1}}\frac{u_2}{e_2}\sqrt{x}$$

$$g_2(x) = x^2$$

$$g_1(1+\alpha_2^{**}u_2) = g_2(1+\alpha_2^{**}u_2).$$

For $x > 0$, we have $g_2''(x) = 2 > 0 > g_1''(x)$. Thus, we have at most two solutions. The transcritical bifurcation through $(\alpha_1, \alpha_2) = (\alpha_1^*, 0)$ happens, if $g_1(1) = g_2(1)$ and $\alpha_1^* > 0$. The condition $g_1(1) = g_2(1)$ reads

$$\frac{u_2}{e_2} < \frac{\sqrt{\frac{u_1}{e_1}}}{1 - e_3\sqrt{\frac{u_1}{e_1}}}.$$

At this line, the condition for positivity of $\alpha_1^{**}(\alpha_2)$ becomes $u_1/e_1 > 1$. This is, a transcritical bifurcation is located at the line $\mathcal{C}_1$.

A second transcritical bifurcation (this time at $(0, \alpha_2^*)$) takes place, if the positivity condition $u_1/e_1 > 1 + \alpha_2 u_2$ breaks down, i.e. for $u_1/e_1 = 1 + \alpha_2 u_2$. We find the corresponding line by inspecting $g_1(u - 1/e_1) = g_2(u_1/e_1)$, and find in this way the line $\mathcal{C}_2$ back. This is, the boundaries of the single-strategy regions $\mathcal{C}_1$ and $\mathcal{C}_2$ form transcritical bifurcations.

We do have an additional bifurcation in the system: a saddle-node bifurcation. The saddle-node bifurcation happens for $g_1(x) = g_2(x)$, $g_1'(x) = g_2'(x)$ at $x = 1 + \alpha_2 u_2 > 1$. The condition $g_1'(x) = g_2'(x)$ reads

$$\sqrt{\frac{e_1}{u_1}}\frac{u_2}{e_2}\frac{1}{2\sqrt{x}} = 2x \;\Rightarrow\; x = \frac{1}{2^{4/3}}\left(\frac{u_1}{e_1}\right)^{-1/3}\left(\frac{u_2}{e_2}\right)^{2/3}.$$

If we plug in this value into $g_1(x) = g_2(x)$, we have

$$-e_3\frac{u_2}{e_2} + \left(\frac{u_1}{e_1}\right)^{-1/2-1/6}\left(\frac{u_2}{e_2}\right)^{1+1/3}\frac{1}{2^{2/3}} = \frac{1}{2^{8/3}}\left(\frac{u_1}{e_1}\right)^{-2/3}\left(\frac{u_2}{e_2}\right)^{4/3}$$

$$\Rightarrow \frac{u_2}{e_2} = \frac{256e_3^3}{27}\left(\frac{u_1}{e_1}\right)^2.$$

The positivity condition for α_1^{**} implies $u_1/e_1 > 1$, while the positivity condition for α_2^{**} corresponds to $x > 1$, this is

$$(u_2/e_2)^2 > 2^{4/3}(u_1/e_2).$$

If $e_3 \in (0,1)$, $e \neq 3/4$, the slope of the saddle-node line is less than that of $\mathcal{C}_2$. Only for

$$e_3 = 3/4$$

the saddle-node line and the transcritical curve $\mathcal{C}_2$ coincide, while $\mathcal{C}_1$ and $\mathcal{C}_2$ are tangential at $(\alpha_1, \alpha_2) = (1, 1/(1-e_3))$. This point is the organizing center of the bifurcation structure. We basically need to understand two parameter intervals: $e_3 \in (0, 3/4)$ and $e_3 \in (3/4, 1)$.

Numerical analysis reveals that for $e_3 > 3/4$ the saddle-node line is not feasible, and we only have one non-trivial two-substrate-solution that connects the one-substrates regions.

For $e_3 \in (0, 3/4)$, the situation is more involving: by means of numerical analysis, one finds that both single-substrate regions overlap. Moreover, from line $\mathcal{C}_1$ a saddle-node bifurcation curve branches (tangentially to this line). In this case, we do have a bistable region with two non-trivial two-substrate solutions, one locally stable and one locally unstable (this is, one local minimum and one local maximum).

Appendix C. Model for batch- and retentostat experiments

Batch culture model. We start off with the energy gain defined in the main part of the paper. Like before, we use time scale arguments to remove the variable T. Letting $\varepsilon_T \to 0$, we obtain

$$B\frac{\alpha_t \mathrm{tol}}{1+\alpha_t \mathrm{tol}} = \mathcal{E}_{t,+} = \frac{\alpha_b T}{1+\alpha_a \mathrm{acetate} + \alpha_b \mathrm{benz} + \alpha_b T}$$

and

$$\begin{aligned} B\alpha_t \mathrm{tol}(1+\alpha_a \mathrm{acetate}+\alpha_b \mathrm{benz}) &= \alpha_b T(1+\alpha_t \mathrm{tol}(1-B)) \\ \Rightarrow (1+\alpha_a \mathrm{acetate}+\alpha_b \mathrm{benz}+\alpha_b T) &= \frac{(1+\alpha_t \mathrm{tol})(1+\alpha_a \mathrm{acetate}+\alpha_b \mathrm{benz})}{(1+\alpha_t \mathrm{tol}(1-B))} \end{aligned}$$

This results leads to the adapted gain functions,

gain (acetate)	$\mathcal{E}_{a,+}$	$= \alpha_a \mathrm{acetate}\frac{1+\alpha_t \mathrm{tol}(1-B)}{(1+\alpha_t \mathrm{tol})(1+\alpha_a \mathrm{acetate}+\alpha_b \mathrm{benz})}$
costs (acetate)	$\mathcal{E}_{a,-}$	$= e_a(\alpha_a - \alpha_a^0)_+$
gain (benzoate)	$\mathcal{E}_{b,+}$	$= \alpha_b \mathrm{benz}\frac{1+\alpha_t \mathrm{tol}(1-B)}{(1+\alpha_t \mathrm{tol})(1+\alpha_a \mathrm{acetate}+\alpha_b \mathrm{benz})}$
costs (benzoate)	$\mathcal{E}_{b,-}$	$= e_b(\alpha_b - \alpha_b^0)_+$
gain (pre-processing toluene)	$\mathcal{E}_{t,+}$	$= \alpha_t \mathrm{tol}/(1+\alpha_t \mathrm{tol})$
costs (toluene)	$\mathcal{E}_{t,1,-}$	$= e_t(\alpha_t - \alpha_t^0)_+$
loss (pre-processing)	$\mathcal{E}_{t,2,-}$	$= \alpha_t \mathrm{tol}/(1+\alpha_t \mathrm{tol})$
Interaction toluene/acetate	$\mathcal{E}_{TA}$	$= \alpha_a \mathrm{tol}/(1+\alpha_a \mathrm{tol})$
Interaction toluene/benzoate	$\mathcal{E}_{TB}$	$= \alpha_b \mathrm{tol}/(1+\alpha_b \mathrm{tol})$

that in turn determine the dynamic model

$$\begin{aligned}
p' &= [A_a\mathcal{E}_{a,+} + A_b\mathcal{E}_{b,+} + A_t\mathcal{E}_{t,+}]p \\
\mathrm{acetate}' &= -B_a\mathcal{E}_{a,+} \\
\mathrm{benz}' &= -B_b\mathcal{E}_{b,+} \\
\mathrm{tol}' &= -B_t\mathcal{E}_{t,+} \\
\mathrm{FeII}' &= \kappa_a B_a\mathcal{E}_{a,+} + \kappa_b B_b\mathcal{E}_{b,+} + \kappa_t B_t\mathcal{E}_{t,+} \\
\varepsilon_a\alpha_a' &= \alpha_a\partial_{\alpha_a}\mathcal{E} \\
\varepsilon_b\alpha_b' &= \alpha_b\partial_{\alpha_b}\mathcal{E} \\
\varepsilon_t\alpha_t' &= \alpha_t\partial_{\alpha_t}\mathcal{E} \\
\mathcal{E} &= \mathcal{E}_{a,+} - \mathcal{E}_{a,-} + \theta_a(\mathcal{E}_{b,+} - \mathcal{E}_{b,-}) + \theta_b(\mathcal{E}_{t,+} - \mathcal{E}_{t,1,-}) \\
&\quad + \psi_{TA}\mathcal{E}_{TA} + \psi_{TB}\mathcal{E}_{TB}.
\end{aligned}$$

The constants ψ_{TA} and ψ_{TB} indicate the relative importance of the cross links between toluene and acetate/benzoate.

Retentostat model. Let D denote the influx/efflux rate, and acet_0, benz_0, and tol_0 the concentration of the three substances in the inflowing medium the model equations then read

$$\begin{aligned}
\mathrm{p}' &= (A_a\mathcal{E}_{+,a} + A_t\mathcal{E}_{+,t} + A_b\mathcal{E}_{+,b})p \\
\mathrm{acetate}' &= D(\mathrm{acetate} - \mathrm{acetate}_0) - B_a\mathcal{E}_{+,a}p \\
\mathrm{benz}' &= D(\mathrm{benz} - \mathrm{benz}_0) - B_t b\mathcal{E}_{+,b}p \\
\mathrm{tol}' &= D(\mathrm{tol} - \mathrm{tol}_0) - B_t\mathcal{E}_{+,t}p \\
\mathrm{FeII}' &= (\kappa_a B_a\mathcal{E}_{+,a} + \kappa_t B_t\mathcal{E}_{+,t} + \kappa_b B_b\mathcal{E}_{+,b})p \\
\varepsilon_a\alpha_a' &= \alpha_a\partial_{\alpha_a}\mathcal{E} \\
\varepsilon_b\alpha_b' &= \alpha_b\partial_{\alpha_b}\mathcal{E} \\
\varepsilon_t\alpha_t' &= \alpha_t\partial_{\alpha_t}\mathcal{E} \\
\mathcal{E} &= \mathcal{E}_{a,+} - \mathcal{E}_{a,-} + \theta_a(\mathcal{E}_{b,+} - \mathcal{E}_{b,-}) + \theta_b(\mathcal{E}_{t,+} - \mathcal{E}_{t,1,-}) + \psi_{TA}\mathcal{E}_{TA} + \psi_{TB}\mathcal{E}_{TB}.
\end{aligned}$$

Parameters of the models. First we list the rate constants of the model. Note that only the rate constant A_a varies between batch culture and retentostat model.

Name	Unit	Value (Batch)	Value (Retento)
A_a	1/h	0.17	0.17 (0.085) (see text below)
e_a	mM	0.1	0.1
θ_A	1	1.2	1.2
B_a	mM/(h cells/ml)	8.4e − 09	8.4e − 09
ε_a	h/mM	40	40
$\alpha_{A,0}$	1/mM	0.01	0.01
A_t	1/h	0.8	0.8
e_t	mM	0.001	0.001
θ_T	1	0.5	0.5
B_t	mM/(h cells/ml)	4e − 09	4e − 09
ε_t	h mM	0.57	0.57
$\alpha_{T,0}$	mM	0.01	0.01
B	1	1	1
A_b	1/h	0.26	0.26
e_b	mM	0.02	0.02
θ_B	1	0.468	0.468
B_b	mM/(h cells/ml)	2e − 09	2e − 09
ε_b	h mM	1	1
$\alpha_{B,0}$	1/mM	0.14	0.14
ψ_{TB}	1	1	1
ψ_{TA}	1	100	100
κ_a	1	8	8
κ_t	1	36	36
κ_b	1	20	20

For replicates "retent. 1", "retent. 3" we used $A_a = 0.085/h$, while for replicates "retent. 2" $A_a = 0.17/h$ was chosen. The initial conditions and D had to be adapted to the experiments (D is zero for batch culture, and given by physical conditions for the retentostat experiments). The following table indicates the values used. Note that only the initial values for the control variables are arbitrary; all other variables have been chosen as indicated by the measurements at the first time point (time zero) resp. the physical conditions of the experiments. To abbreviate notations, we denote in the batch experiments by bath 1 the experiment with acetate only, by batch 2 the experiment with benzoate only, by batch 3 that with benzoate and toluene, and by batch 4 that with acetate and toluene.

Variable	unit	batch 1	batch 2	batch 3	batch 4	retent. 1	retent. 2	retent. 3
acetate	mM	3.7	0	0	2.5	0	1.3	1.3
benz	mM	0	0.7	0.35	0.5	0	0.3	0.45
tol	mM	0	0	0.4	0	0	0	0
p	1e6 cells/ml	6.65	6.65	6.65	6.65	120	75	288
FeII	mM	3.6	4.5	0.9	0.325	37	0	35
α_A	1/mM	0.01	0.01	0.01	0.01	0.4	0.8	0.06
α_B	1/mM	0.01	0.01	0.01	0.01	0.8	0.08	7e−5
α_T	1/mM	0.01	0.01	0.01	0.01	0.01	0.01	0.01
acetate_0	mM	–	–	–	–	2.5	2.5	2.5
benz_0	mM	–	–	–	–	0.7	0.7	0.7
tol_0	mM	–	–	–	–	0	0	0
D	ml/h	–	–	–	–	30	30	30

References

[1] K. Bettenbrock, S. Fischer, A. Kremling, K. Jahreis, T. Sauter, E.-D. Gilles, A quantitative approach to catabolite repression in *Escherichia coli*, J. Biol. Chem. 281 (2006) 2578–2584.
[2] J. Butler, Q. He, K. Nevin, Z. He, J. Zhou, D. Lovley, Genomic and microarray analysis of aromatics degradation in *Geobacter metallireducens* and comparison to a Geobacter isolate from a contaminated field site, BMC Genom. 8 (2007) 189.
[3] C. Chassagnole, N. Noisommit-Rizzi, J.W. Schmid, K. Mauch, M. Reuss, Dynamic modeling of the central carbon metabolism of *Escherichia coli*, Biotechnol. Bioeng. 79 (1) (2002) 53–73.
[4] M.W. Covert, B. Palsson, Transcriptional regulation in constraints-based metabolic models of *Escherichia coli*, J. Biol. Chem. 277 (31) (2002) 28058–28064.
[5] I.G. de Jong, P. Haccou, O.P. Kuipers, Bet hedging or not? A guide to proper classification of microbial survival strategies, BioEssays 33 (3) (2011) 215–223.
[6] E. Dekel, U. Alon, Optimality and evolutionary tuning of the expression level of a protein, Nature 436 (2005) 588–592.
[7] T. Egli, Growth kinetics, bacterial, in: Encyclopedia of Microbiology, Oxford, 2009, pp. 180–193.
[8] T. Egli, Nutrition, in: Encyclopedia of Microbiology, Oxford, 2009, pp. 180–193.
[9] S. Freilich, A. Kreimer, E. Borenstein, N. Yosef, R. Sharan, U. Gophna, E. Ruppin, Metabolic-network-driven analysis of bacterial ecological strategies, Genome Biol. 10 (6) (2009) R61.
[10] W.C. Fuqua, S.C. Winans, E.P. Greenberg, Quorum sensing in bacteria: the LuxR–LuxI family of cell density-responsive transcriptional regulators, J. Bacteriol. 176 (1994) 269–275.
[11] U. Gerland, T. Hwa, Evolutionary selection between alternative modes of gene regulation, PNAS (2009).
[12] B. Görke, J. Stülke, Carbon catabolite repression in bacteria: many ways to make the most out of nutrients, Nat. Rev. Microbiol. 6 (2008) 613–624.
[13] B. Hense, C. Kuttler, J. Müller, M. Rothballer, A. Hartmann, J.-U. Kreft, Does efficiency sensing unify diffusion and quorum sensing?, Nat Rev. Microbiol. 5 (2007) 230–239.
Q7 [14] W. Holms, Control of flux through the citric acid cycle and the glyoxylate bypass in *Escherichia coli*, Biochem. Soc. Symp. 54 (1986) 17–31.
[15] F. Jacob, J. Monod, Genetic regulatory mechanisms in the synthesis of proteins, J. Mol. Biol. 3 (1961) 318–356.
[16] H. Kacser, J.A. Burns, H. Kacser, D.A. Fell, The control of flux, Biochem. Soc. Trans. 23 (1995) 341–366.
[17] T. Kalisky, E. Dekel, U. Alon, Costbenefit theory and optimal design of gene regulation functions, Phys. Biol. 4 (4) (2007) 229.
[18] J.-H. Kim, D. Block, D. Mills, Simultaneous consumption of pentose and hexose sugars: an optimal microbial phenotype for efficient fermentation of lignocellulosic biomass, Appl. Microbiol. Biotechnol. 88 (5) (2010) 1077–1085.
[19] J.-H. Kim, S.P. Shoemaker, D.A. Mills, Relaxed control of sugar utilization in *Lactobacillus brevis*, Microbiology 155 (4) (2009) 1351–1359.
[20] D.S. Kompala, D. Ramkrishna, N.B. Jansen, G.T. Tsao, Investigation of bacterial growth on mixed substrates: experimental evaluation of cybernetic models, Biotechnol. Bioeng. 28 (7) (1986) 1044–1055.
[21] B. Lin, H.V. Westerhoff, W.F.M. Rling, How Geobacteraceae may dominate subsurface biodegradation: physiology of *Geobacter metallireducens* in slow-growth habitat-simulating retentostats, Environ. Microbiol. 11 (9) (2009) 2425–2433.
[22] D. López, R. Kolter, Extracellular signals that define distinct and coexisting cell fates in *Bacillus subtilis*, FEMS Microbiol. Rev. 34 (2) (2010) 134–149.
[23] D. Lovley, S. Giovannoni, D. White, J. Champine, E. Phillips, Y. Gorby, S. Goodwin, *Geobacter metallireducens* gen. nov. sp. nov., a microorganism capable of coupling the complete oxidation of organic compounds to the reduction of iron and other metals, Arch. Microbiol. 159 (4) (1993) 336–344.
[24] L. Lynd, P. Weimer, W. van Zyl, I. Pretorius, Microbial cellulose utilization: fundamentals and biotechnology, Microbiol. Mol. Biol. Rev. 66 (2002) 506–577.
[25] S. Marozava, W.F.M. Röling, J. Seifert, R. Köffner, M. von Bergen, R.U. Meckenstock, Physiology of *Geobacter metallireducens* under excess and limitation of electron donors. Part I. Batch cultivation with excess of carbon sources, Syst. Appl. Microbiol. 37 (2014) 277–286.
[26] S. Marozava, W.F.M. Röling, J. Seifert, R. Köffner, M. von Bergen, R.U. Meckenstock, Physiology of *Geobacter metallireducens* under excess and limitation of electron donors. Part II. mimicking environmental conditions during cultivation in retentostats, Syst. Appl. Microbiol. 37 (2014) 287–295.
[27] J. Metz, S. Mylius, O. Diekmann, When does evolution optimize?, Evol Ecol. Res. 10 (2008) 629–654.
[28] J. Monod, Recherches sur la croissance des cultures bactériennes, Hermann et Cie, Paris, 1942.
[29] J. Müller, B. Hense, T. Fuchs, M. Utz, C. Pötzsche, Bet-hedging in stochastically switching environments, J. Theor. Biol. 336 (2013) 144–157.
[30] P.I. Nikel, R. Silva-Rocha, I. Benedetti, V. de Lorenzo, The private life of environmental bacteria: pollutant biodegradation at the single cell level, Environ. Microbiol. (2013).
[31] M.R. Parsek, E. Greenberg, Sociomicrobiology: the connections between quorum sensing and biofilms, Trends Microbiol. 13 (2004) 27–33.
[32] S. Quan, C. Ray, Z. Kwota, T. Duong, G. Balázsi, T. Cooper, R. Monds, Adaptive evolution of the lactose utilization network in experimentally evolved populations of *Escherichia coli*, PLoS Genet. 8 (2012) e1002444.
[33] R. Rabus, Functional genomics of an anaerobic aromatic-degrading denitrifying bacterium, strain EbN1, Appl. Microbiol. Biotechnol. 68 (5) (2005) 580–587.
[34] R. Ramakrishna, D. Ramkrishna, A.E. Konopka, Cybernetic modeling of growth in mixed, substitutable substrate environments: preferential and simultaneous utilization, Biotechnol. Bioeng. 52 (1) (1996) 141–151.
[35] M. Santillán, M.C. Mackey, Quantitative approaches to the study of bistability in the lac operon of *Escherichia coli*, J. Roy. Soc. Interf. 5 (Suppl 1) (2008) S29–S39.
[36] S.J. Schreiber, G.A. Tobiason, The evolution of resource use, J. Math. Biol. 47 (1) (2003) 56–78.
[37] J.-S. Seo, Y.-S. Keum, Q. Li, Bacterial degradation of aromatic compounds, Int. J. Environ. Res. Public Health 6 (2009) 278–309.
[38] K.D. Singh, M.H. Schmalisch, J. Stlke, B. Grke, Carbon catabolite repression in *Bacillus subtilis*: quantitative analysis of repression exerted by different carbon sources, J. Bacteriol. 190 (21) (2008) 7275–7284.

Q1 Please cite this article in press as: J. Müller et al., Model selection for microbial nutrient uptake using a cost-benefit approach, Math. Biosci. (2014), http://dx.doi.org/10.1016/j.mbs.2014.06.012

[39] E. Sintes, G.J. Herndl, Quantifying substrate uptake by individual cells of marine bacterioplankton by catalyzed reporter deposition fluorescence in situ hybridization combined with microautoradiography, Appl. Environ. Microbiol. 72 (11) (2006) 7022–7028.
[40] H. Smith, P. Waltman, The Theory of the Chemostat, Cambridge University Press, 1995.
[41] J.V. Straight, D. Ramkrishna, Cybernetic modeling and regulation of metabolic pathways. Growth on complementary nutrients, Biotechnol. Progr. 10 (6) (1994) 574–587.
[42] J. Sun, B. Sayyar, J. Butler, P. Pharkya, T. Fahland, I. Famili, C. Schilling, D. Lovley, R. Mahadevan, Genome-scale constraint-based modeling of *Geobacter metallireducens*, BMC Syst. Biol. 3 (1) (2009) 15.
[43] F. Titgemeyer, W. Hillen, Global control of sugar metabolism: a gram-positive solution, Anton. Leeuw. 82 (1–4) (2002) 59–71.
[44] B. Tropp, Molecular Biology: Genes to Proteins, Jones & Bartlett, 2011.
[45] D. Walton, B.P. Leard, A. Tongen, An optimal strategy for energy allocation in a multiple resource environment, Bull. Math. Biol. 72 (5) (2010) 1092–1123.
[46] J. Wang, E. Gilles, J. Lengeler, K. Jahreis, Modeling of inducer exclusion and catabolite repression based on a PTS-dependent sucrose and non-PTS-dependent glycerol transport systems in *Escherichia coli* K-12 and its experimental verification, J. Biotechnol. 92 (2001) 133–158.
[47] S. Wischgoll, D. Heintz, F. Peters, A. Erxleben, E. Sarnighausen, R. Reski, A. Van Dorsselaer, M. Boll, Gene clusters involved in anaerobic benzoate degradation of *Geobacter metallireducens*, Mol. Microbiol. 58 (5) (2005) 1238–1252.
[48] P. Wong, S. Gladney, J.D. Keasling, Mathematical model of the lac operon: inducer exclusion, catabolite repression, and diauxic growth on glucose and lactose, Biotechnol. Progr. 13 (2) (1997) 132–143.

Q1 Please cite this article in press as: J. Müller et al., Model selection for microbial nutrient uptake using a cost-benefit approach, Math. Biosci. (2014), http://dx.doi.org/10.1016/j.mbs.2014.06.012